UNCLASSIFIED

AD NUMBER

AD818134

LIMITATION CHANGES

TO:

Approved for public release; distribution is unlimited.

FROM:

**Distribution authorized to U.S. Gov't. agencies and their contractors;
Administrative/Operational Use; 31 JUL 1967.
Other requests shall be referred to Office of Naval Research, Arlington, VA 22203.**

AUTHORITY

ONR ltr 27 Jul 1971

THIS PAGE IS UNCLASSIFIED

AD818134

BEST
AVAILABLE COPY

MISSING PAGE
NUMBERS ARE BLANK
AND WERE NOT
FILMED

PERKIN-ELMER

STATEMENT #2 UNCLASSIFIED

This document is subject to special export controls and each transmittal to foreign governments or foreign nationals may be made only with prior approval of ONR, Code 421 Wash DC 20360

THE PERKIN-ELMER CORPORATION
(Report No. 8884)
ABSORPTION OF LIGHT IN GASES

Final Report
Through 31 July 1967

Submitted by

Earl L. Sloan III, Project Scientist
(Phone No. 203-762-4727)
and
Edwin L. Kerr
(Phone No. 203-762-4650)

to the

OFFICE OF NAVAL RESEARCH

"Reproduction in Whole or in Part of this Report is Permitted for any Purpose of The United States Government."

This Research is part of Project DEFENDER under the joint sponsorship of the Advanced Research Projects Agency, the Office of Naval Research, and the Department of Defense.

Contract No. Nonr-4661(00)
1 November 1964 Through 31 July 1967

TABLE OF CONTENTS

TABLE OF CONTENTS (Continued)

LIST OF ILLUSTRATIONS

ABSTRACT

Two methods of measuring optical molecular absorptivities in gases, potentially capable of approaching theoretical sensitivity limits of 10^{-8} cm^{-1} were studied. An acoustic method was pushed experimentally to a sensitivity of 10^{-5} cm^{-1} absorptivity. Practical obstacles to further improvement have been found for the acoustic method. The second method, a laser illuminated "spectrophone", was also investigated. Its performance was much closer to the theoretical limit.

The acoustic method is only suitable for use with a pulsed source laser. We used a Q-switched ruby laser, tunable from pulse to pulse over a 2Å range, as the excitation source. Absorbed light causes a temperature rise and expansion of the gas sample. The expansion starts cylindrically propagating sound disturbances. These are focused by acoustic mirrors onto a membrane detector. The membrane is one reflector of a near confocal resonator, illuminated by a frequency stable gas laser. Small membrane displacements are detected as fringe motion across a sensing prism by two photomultiplier tubes. Large displacements are averted by a servo loop which applies the photomultiplier difference signal to electric grids, forcing the membrane to stay within one order of the resonator. The loop feedback signal is a calibratable measure of the gas optical molecular absorptivity at the wavelength of the ruby laser pulse.

One practical problem of the acoustic method is the high frequency and transient nature of the signal. The longest wavelength is twice the laser beam diameter, so the signal frequencies are 300 kHz and higher. The membrane must be very thin to respond to such high frequencies and its displacement is typically less than 1Å. The membrane reflectivity cannot be made greater than

60 percent, so the resonator fringes have low finesse. These practical difficulties make shot noise in the fringe-reading photometer, rather than Brownian noise, the limit of performance.

In the spectrophone method the gas sample is enclosed in a sealed tube. The gas expansion causes a pressure rise which is transmitted to the pressure transducer through a short duct. High frequency problems are avoided. The observation time is typically 30 milliseconds, set by thermal diffusion from the gas sample to the tube walls. Laser source excitation provides sufficient radiation to measure very weak absorptivities precisely. This report describes the theoretical capability, design considerations, and experimental testing of a pulsed ruby laser spectrophone and a CW CO_2 spectrophone. A spectrum of the water vapor line at 6943.8A was obtained. The peak absorptivity was 3×10^{-6} cm^{-1}. Near 9.6 microns, absorptivities of CO_2 - N_2 mixtures were measured down to 1.2×10^{-7} cm^{-1}.

SECTION I

INTRODUCTION

1.1 CONVENTIONAL MEASURING METHODS

Broadband optical absorption of the whole atmosphere has been studied in considerable detail, because of its relevance to astronomy. Sunlight provides a strong, almost continuous source, and high resolution can be obtained. Babcock and Moore[1] have published considerable data on atmospheric transmission and have identified many of the absorptions as either atmospheric or solar. More recently, data have been taken for the lower atmosphere, using a tungsten source. The atlas, published by Curcio, Drummeter, and Knestrick,[2] was obtained over a 16 km uncontaminated air path, using a 1000 watt tungsten lamp as the source. In this study, the spectrum of the source can be measured independently of the sample. The absorbing sample itself consists of molecular oxygen and water vapor.

Atmospheric absorption in the vicinity of laser lines has become important recently because of the advent of terrestrial laser communications and radars, and because of the eventual application of lasers in space communications. Ronald Long[3] took a high resolution spectrum of atmospheric absorption in the tunable range of ruby lasers on a cold, clear winter day. He has also attempted to observe absorption in a 50 foot cell with a 1 km path[4]. His results indicate an absorptivity of less than 10^{-7} cm^{-1} in air near 6943 Å (694.3 nm).

1.2 THE GOAL: A DIRECT METHOD

Precise quantitative measurements of light absorption in small gas samples are difficult to achieve with conventional, indirect spectroscopic methods. Typical optical molecular absorptivities may be 10^{-6} cm^{-1} and have bandwidths of less than 0.03 wavenumbers at atmospheric pressures. Detection of trace constituents presents an even more formidable problem. Laboratory

techniques may be subject to large experimental errors, because either they involve measuring the intensity difference of two nearly equal source beams, or the source makes multiple reflections in the sample cell and the experimental error in measuring the reflectivity is compounded. When atmospheric transmission over long air paths is measured, there is little control of the sample.

The goal of this research was to develop a direct method of measuring absorption. By "direct" we mean a method dependent on the energy absorbed by the gas, as opposed to methods which depend on the difference of source and transmitted energy. Culver[5], in a brief paper, suggested an acoustic method using a tunable pulsed laser as a source. In Culver's proposal, the absorbed energy causes a pressure rise in the gas sample, and the resulting sound wave is focused to a microphone by a cylindrical cavity of elliptical cross section. The microphone signal is proportional to the absorption. The limiting sensitivity Culver calculates is $3 \times 10^{-11} cm^{-1}$ absorption, assuming Brownian pressure fluctuation is the limiting noise. Thus, while Culver's acoustic method appears feasible, we show in the section on Brownian noise pressure and displacement that the limiting noise of a practical microphone for the acoustic method is much greater than Brownian noise. We believe there is little hope of adequate improvement of the microphone, for reasons detailed later.

1.3 EVALUATION OF TWO DIRECT METHODS

In the first year of work, we completed an experimental and theoretical evaluation of our version of the acoustic method as a means of measuring absorption of light in gases. In the acoustic method we explored, the sound mirrors are a paraboloid and a cylindrical parabola, so the sound is focused to a point rather than along a line. We developed a sensitive, high frequency membrane microphone as a detector. The system was pushed to a sensitivity of $10^{-5} cm^{-1}$ absorptivity. However, the technical problems described in the section on the acoustic method make the whole system less attractive than the spectrophone system we developed later. The acoustic method does appear to be useful for studying molecular absorption relaxation times in the 10 to 100 microsecond range, provided the sample absorptivity is greater than about $10^{-4} cm^{-1}$ and there is a pulsed laser source to match them.

In the spectrophone method, the gas sample is enclosed in a cylindrical sample cell with end windows whose transmission characteristic is appropriate to the source laser. The cell radius fits the beam radius more or less closely, but not so closely that laser light incident on the tube sidewalls will cause strong desorption. A short duct connects the sample chamber to the pressure transducer. The MKS Baratron, which is a sealed capacitor microphone is used. For a pulsed laser, the measuring bandwidth is limited by the pressure decay time constant as the heat is dissipated in the tube walls. For a CW laser, a square-wave chopping frequency may be chosen which matches the time constant for attaining the steady-state pressure. The energy or power, and the laser wavelength, are recorded along with the pressure signal.

The spectrophone method has been applied successfully with both the CO_2 laser near 9.6 microns, and the ruby laser. Absorptivities as weak as $10^{-7}cm^{-1}$ have been measured. With simple refinements of our first spectrophone breadboards, we believe the system is capable of measuring absorptivities of $10^{-8}cm^{-1}$ to within ±10%.

1.4 PLAN OF THE REPORT

Sections II through V describe the acoustic method, analyze its limitations, set forth the important design considerations, review the experimental effort, and give our evaluation of the method.

Appendices B and C are a draft of an article we expect to publish shortly. It is a theoretical and experimental documentation of the spectrophone method.

SECTION II

THEORETICAL LIMITATIONS OF THE ACOUSTIC METHOD

2.1 DESCRIPTION OF THE ACOUSTIC METHOD

Refer to Figure 1 for a schematic layout of the acoustic method for measuring optical absorptivities in gases. The pulsed laser fires through a gas sample contained in the acoustic chamber. Laser wavelength is varied by cooling the pulsed laser with a temperature control system. An energy monitor system (not shown) records the relative energy of each laser burst.

Light absorption causes the gas in the laser beam to expand suddently. The resulting sound wave is captured by the parabolic cylindrical reflector and focused by the paraboloidal reflector onto the microphone diaphragm.

The diaphragm is a thin collodion membrane. It forms one end of the optical resonator associated with a single mode gas laser. This second laser is distinct from the pulsed laser. Vibrations of the membrane in response to the acoustic pulses cause the resonant beam of the laser to shift position on the nose of a sensing prism. The resulting signal imbalance from a pair of photodetectors is amplified and displayed on the oscilloscope for photographically recording the amplitude of the acoustic pulse.

2.2 SIGNAL BANDWIDTH AND EXTRANEOUS NOISE SOURCES

The frequency band and observation time of the signal play a very important part in the reduction of extraneous noise. If the measuring system is optical, it will be shot-noise limited unless the signal observation time is sufficiently long to permit integration of the photomultiplier signal. A capacitor microphone may be limited by Johnson noise if the signal bandwidth is too great. On the other hand, if the observation time is too long, the

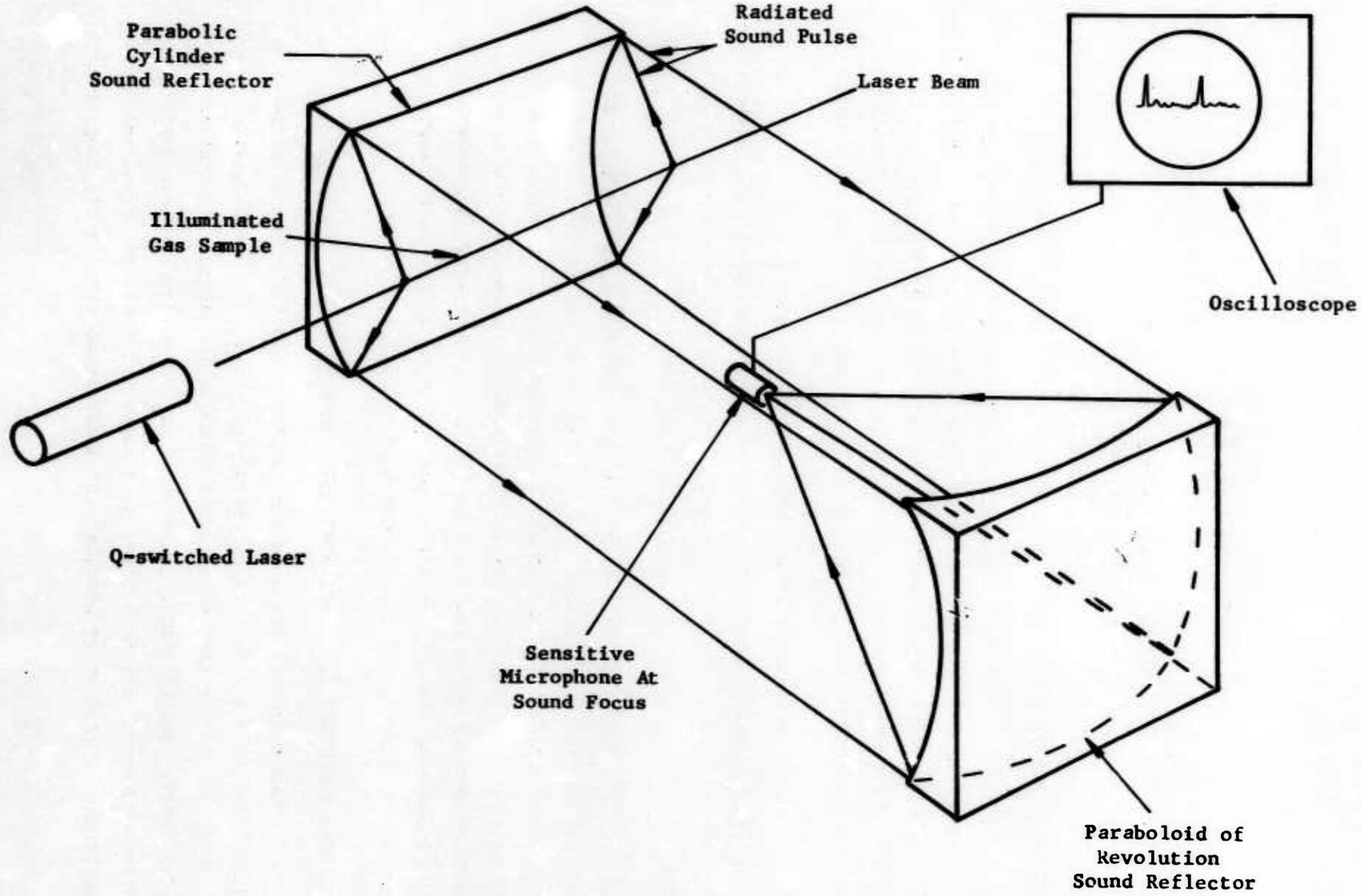

Figure 1. The Acoustic Method for Measuring the Absorption of Light in Gases

measuring apparatus must be stabilized against thermal drift. Obviously, the measuring device employed must be matched to the signal bandwidth.

2.3 BROWNIAN NOISE PRESSURE AND DISPLACEMENT

The signal pressure rise is given by the heat capacity C_V of the gas and the ideal gas law. The pressure rise $p = P J \alpha/C_V T$. Signal and noise pressures in db may be calculated from $20 \log_{10} (p/p_o)$, where $p_o = 2 \times 10^{-4}$ dynes/cm^2 = Brownian noise pressure in a 19 kHz bandwidth. When we come to a practical device however, a signal-to-noise ratio calculated from pressure ratios may be misleading. Most microphones are displacement or velocity sensitive, not truly pressure sensitive. Some idea of microphone element displacement may be obtained from the free sound field displacement, which decreases inversely as frequency. If y is the displacement and p is the (relative) sound pressure;

$$y = p/2 \pi f \rho_o v$$

For air, the density $\rho_o = 0.00122$ gram/cm^3 and the speed of sound, v, is 34,600 cm/sec. Thus, if $p = 10^{-2}$ dynes/cm^2, and if f = 40 kHz, y = 0.94Å. (It is possible to have average sound displacements of less than an atomic diameter. Displacement itself is a macroscopic concept.)

2.4 ACOUSTIC IMPEDANCE MATCHING

If the sound wave impinges on a material with much greater acoustic impedance than air, the surface of the material will undergo much less displacement than the free sound field displacement; i.e., the material is not well coupled to the air. For good coupling at the sound frequency, f, the microphone diaphragm should have much less mass than a column of air whose cross-sectional area is the same as the diaphragm and whose length is L = v/f. Also, any other sound reflector surfaces must be several sound wavelengths from the diaphragm when there is a dispersion of sound frequencies. This latter requirement eliminates capacitor microphones from consideration. We must use optical means for reading the diaphragm displacement.

SECTION III

PRELIMINARY DESIGN CONSIDERATIONS FOR THE ACOUSTIC METHOD

3.1 MEMBRANE REQUIREMENTS

In the acoustic method a microphone response time of 3 microseconds to 30 microseconds is required. This places a severe restriction on the membrane. The membrane may be only about 0.1 micron thick, and have a very thin metallic coating. We selected collodion for the membrane material in the acoustic method, because it can be cast to a thickness of 0.1 micron to 0.2 micron. The only metal that can be mirror coated on such thin collodion is antimony. Reflectivities as high as 60 percent can be obtained.

3.2 MEMBRANE FREQUENCY RESPONSE

A free membrane microphone has smooth response only below the resonance frequency, which is $\nu_{01} = (0.38/a)\ (T/\sigma)^{1/2}$ for a circular membrane of radius a, tension T, and surface density σ. The tension must be high for good frequency response and surface flatness. However, in the acoustic method, it is not possible to obtain high enough tension in any membrane material to operate below the resonance frequency with a membrane large enough to capture the main lobe of the sound diffraction pattern. We therefore used a large membrane of 8 mm radius to reduce the high eigenfrequency spacing.

3.3 PRACTICAL LIMITS TO MEMBRANE REFLECTIVITY

For good coupling and high frequency response the membrane must have low mass. However, high reflectivity requires a flat, smooth surface for depositing metallic or multilayer dielectric films. The deposition process may subject the membrane to high temperatures, depending on the material to be deposited. If the membrane is too thin, it will wrinkle or vaporize when the coating is applied. Thus, the requirements of high frequency response and high reflectivity are in conflict.

The best results we have obtained in our experiments have been a reflectivity of 60 percent for antimony-coated collodion and a finesse of about 2 for the high frequency microphone. We believe that the collodion reflectivity cannot be improved significantly because collodion cannot withstand high temperatures.

3.4 FINESSE AND VISIBILITY

The effect of reflectivity on finesse of a Fabry-Perot etalon or confocal resonator is shown in Figure 2. The relevant reflectivity is the geometric mean of the reflectivities of the two end faces of the etalon. Finesse, the ratio of peak spacing to peak half width, decreases sharply as the reflectivity drops below 90 percent. Above 90 percent reflectivity, the finesse is approximately $\pi R^{1/2}/(1-R)$. High finesse is obviously important for detecting small fringe motions.

The maximum intensity of the fringes depends on how the etalon is illuminated and viewed. If one end of the etalon is a metallized membrane, the absorbance of the coating is usually too large to permit viewing the fringes by transmission.

When the fringes are viewed by reflection, the design problem is as follows: To make the membrane reflectivity as high as possible consistent with the requirements of low mass, flatness, and the ability of membrane material to withstand heat; and then to choose a dielectric coating for the other mirror whose reflectivity is a compromise between high finesse and visibility.

3.5 CONFOCAL RESONATOR DESIGN FOR THE MEMBRANE MICROPHONE

For high frequency response, we must keep a large air space between the membrane and the glass end of the resonator, so the membrane can follow the free sound field. This means the resonator must be designed as a near-confocal resonator. It is not possible to illuminate the resonator on-axis, because light reflected by the curved mirror will couple back with the stable gas laser, even if a quarter-wave plate is used. There are off-axis

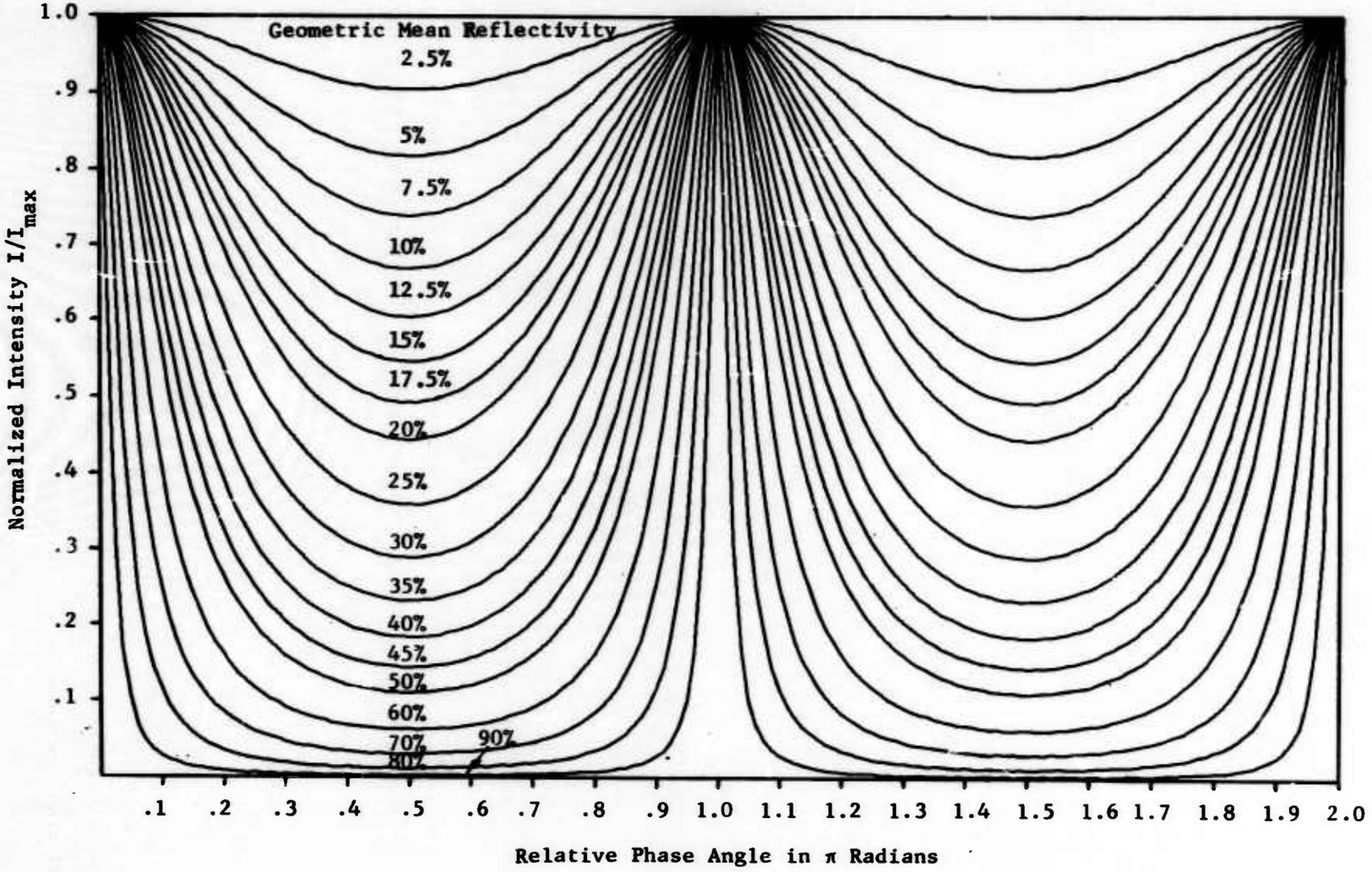

Figure 2. Intensity Distribution for Multiple Beam Fringes Normalized to Unit Intensity

circulator modes for a folded near-confocal resonator, but they involve too many reflections to have good finesse. The configuration of Figure 3 solves these problems. Outside the resonator it has all the properties of an off-axis circulator mode. Inside the resonator, the biprism makes the spherical mirror appear to be two spherical mirrors tilted at a slight angle to each other, with apparent virtual centers as shown by the open circles behind the membrane. It appears to be a folded resonator. The light reflected from the back of the sphere does not reenter the gas laser and can also be kept away from the fringes.

3.6 ACOUSTIC SIGNAL ATTENUATION

In the acoustic method one must consider acoustic absorption as the pressure wave is focused on the microphone. Normally acoustic attenuation increases inversely with the square of frequency. In air there is also an anomalous acoustic absorption, amounting to 20 nepers per meter at 10^6 Hz. This indicates that the acoustic focusing path can be no greater than 50 cm, and the frequencies must be much lower than 10^6 Hz. The frequencies are set by the beam diameter; the lowest one has a wavelength about twice the beam diameter. Thus, for 300 kHz signals, the beam radius is about 1 mm.

The "clam shell" configuration that we chose for the sample chamber and acoustic focusing system has a sample length of 30 cm and a path length of 50 cm. It is shown in Figure 4. There is a cylindrical parabolic sound mirror to reflect the pressure signal as a plane wave, and an f/2 paraboloid to focus it on the microphone. These sound mirrors are shown in Figures 5 and 6.

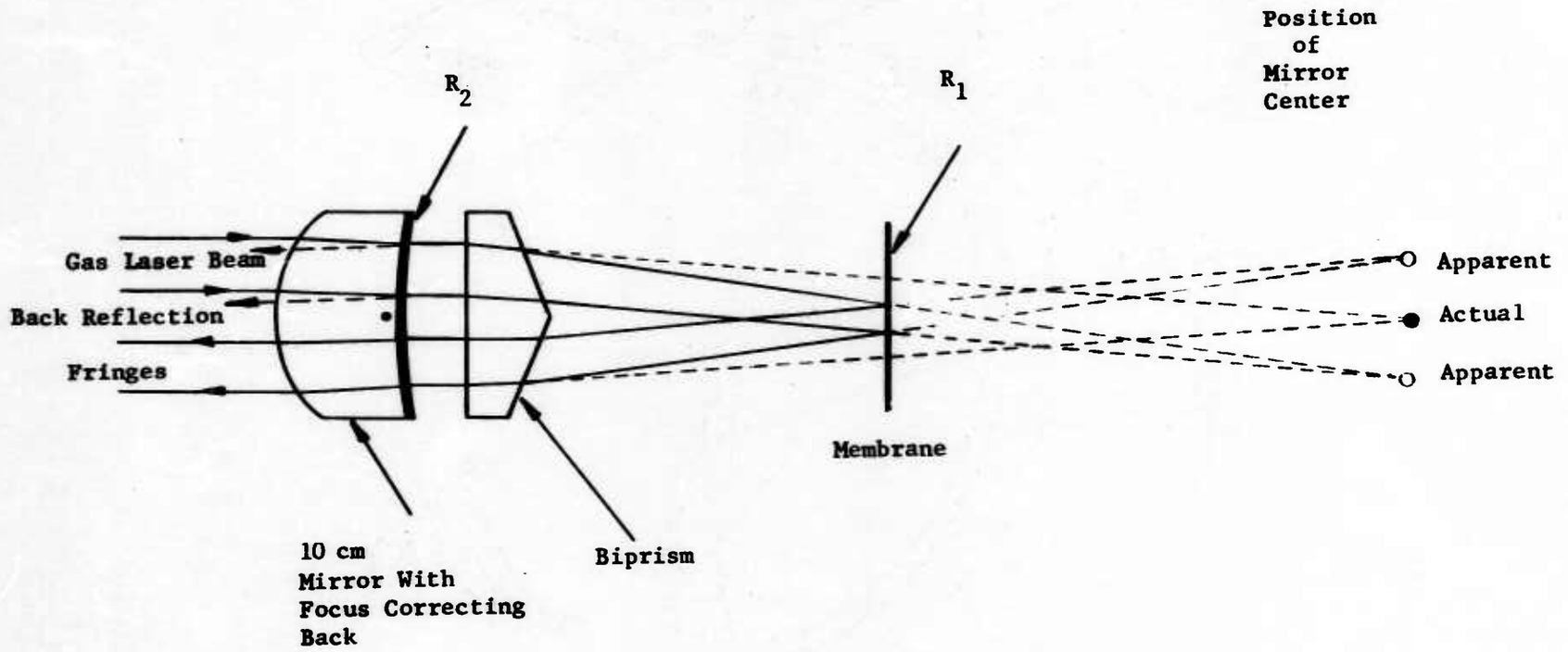

Figure 3. Folded Off-Axis Near-Confocal Resonator With Biprism Corrector

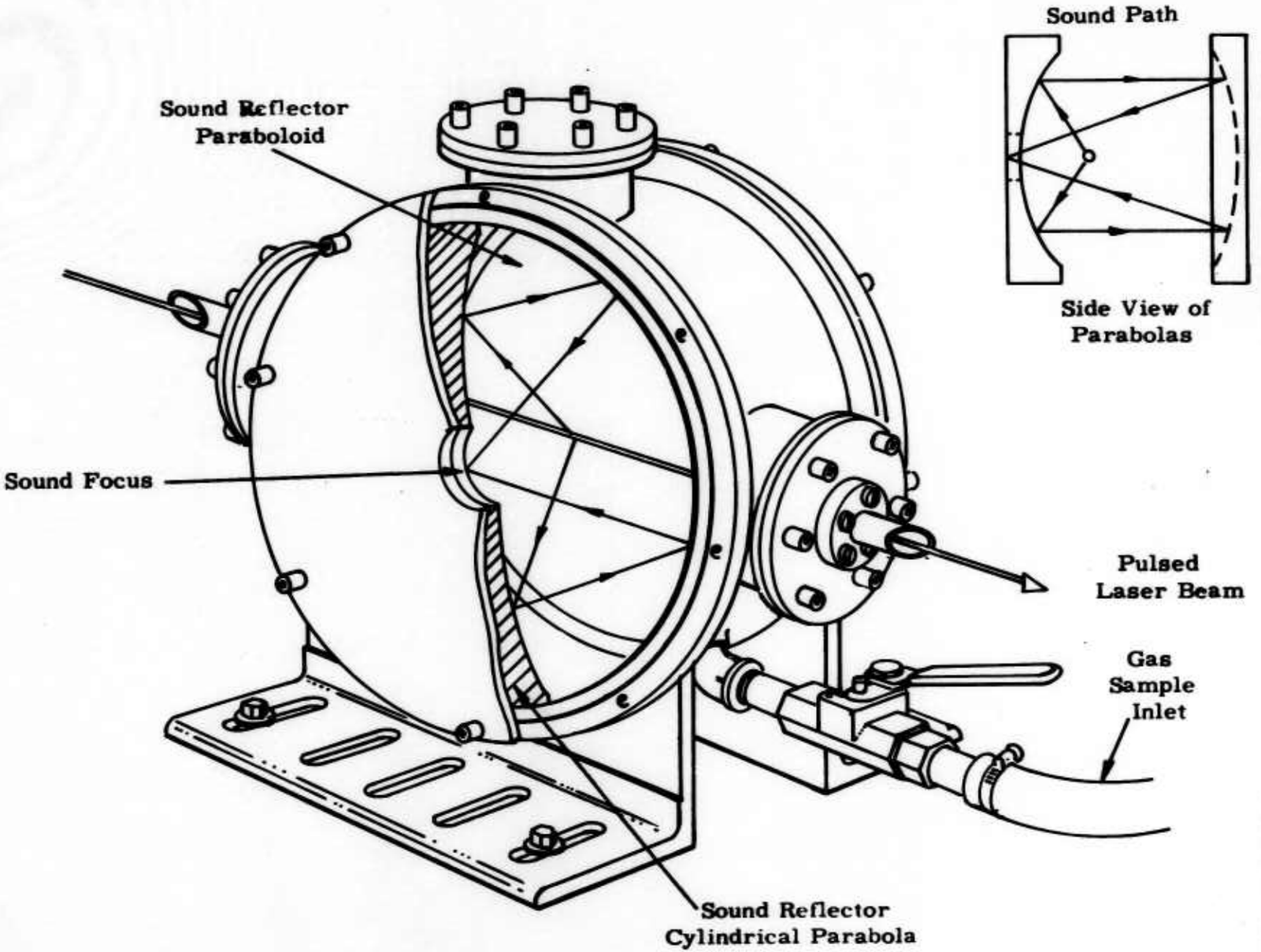

Figure 4. Acoustic Chamber

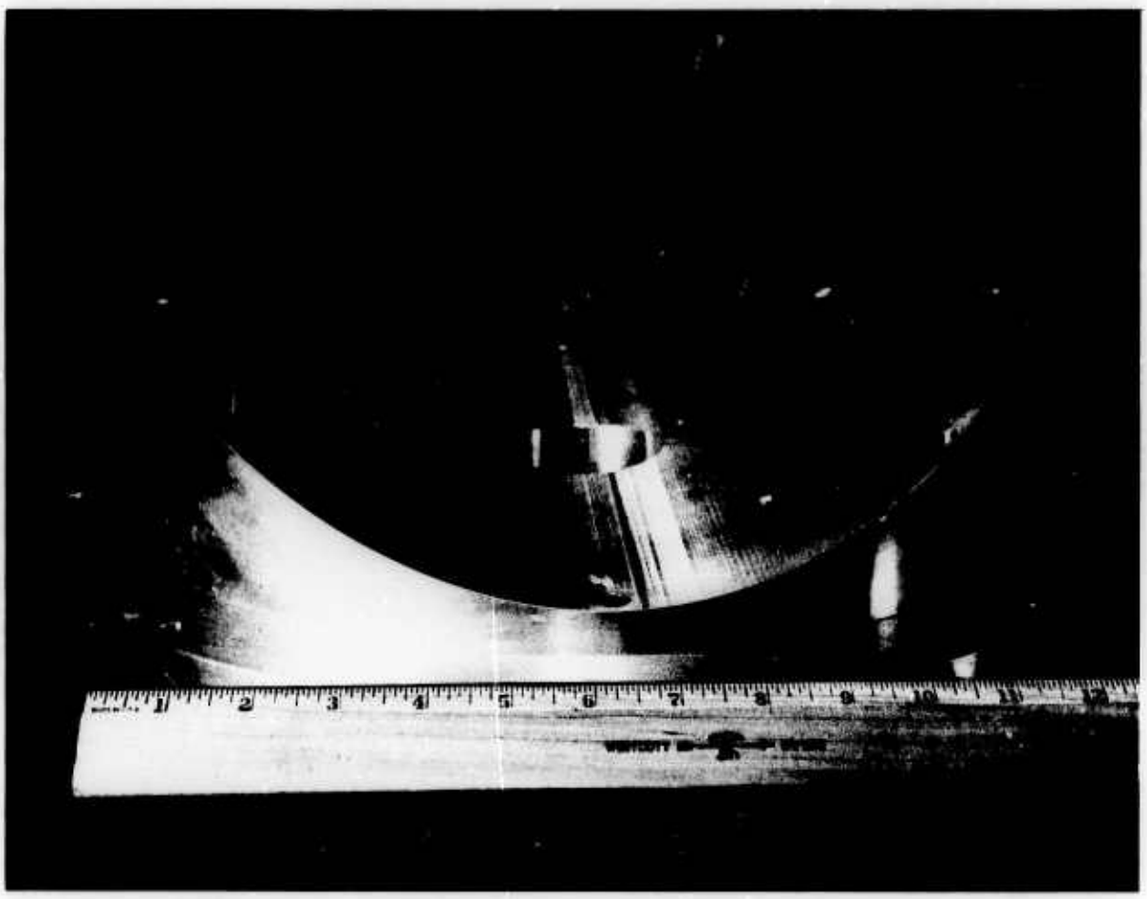

Figure 5. Cylindrical Parabolic Sound Mirror

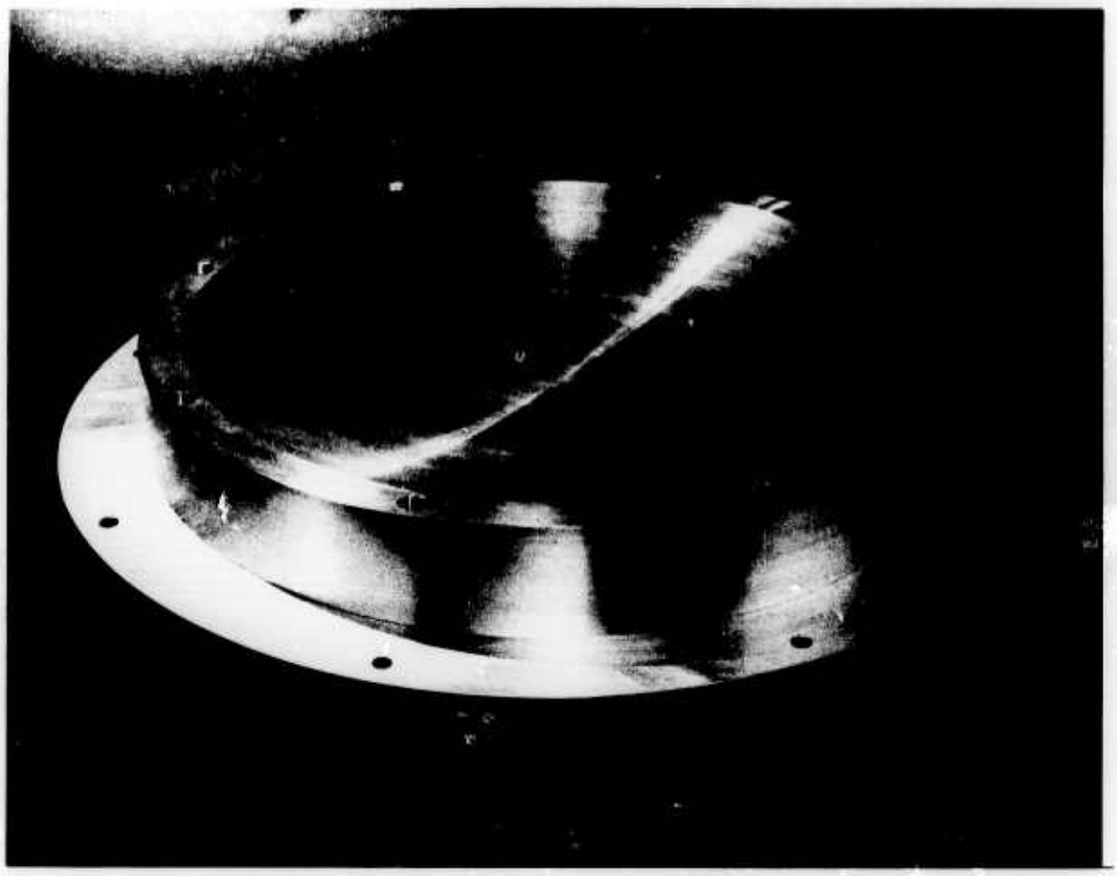

Figure 6. Paraboloidal Sound Mirror

SECTION IV

EXPERIMENTS AND RESULTS WITH THE ACOUSTIC METHOD

4.1 HIGH FREQUENCY MICROPHONE BREADBOARD

In the original conception of the high frequency microphone, the output signal was not applied to force balancing grids. Our intention was to shift the wavelength of the gas laser emission in response to spurious low frequency signals. This was to provide a stable operating point. The observed signal would be high frequency excursions from this point. The gas laser is constructed with a piezoelectric pusher on one of its cavity mirrors. The frequency response of the pusher is roughly 0 to 1 kHz. The pusher may be moved through seven orders of the gas laser cavity.

In our initial breadboard a collodion membrane of 1 cm diameter coated with antimony to about 50 percent reflectivity was used. The other resonator mirror had a 30 cm radius of curvature. A small lens of about 30 cm focal length was used to correct the negative power of the flat-backed spherical mirror. We set up the system in a straight, on-axis resonant mode. The order of elements was the gas laser, the corrector lens, the 30 cm mirror, the membrane, and a photocell.

The observed signal was the resonator intensity pattern being driven rapidly back and forth by room noise. We measured the room noise at 50 db relative to 2×10^{-4} dynes cm^{-2}. When we attempted to close the servo loop to the gas laser pusher, we found that no locking on a single order could be achieved because the sounds of higher frequency than 1 kHz were able to drive the membrane through orders of the 15 cm resonator. The pusher frequency response cannot be improved significantly because of the high capacity of the piezoelectric wafers.

This problem of high frequency dynamic range led to development of the force-balance microphone.

4.2 FORCE BALANCE MICROPHONE BREADBOARD

We next constructed the first force balance microphone. The collodion-antimony membranes of 1 cm diameter were used. The wire grids were situated 1 mm from each side of the membrane. A 1500 volt bias could be applied (at atmospheric pressure) without breakdown or corona.

Various methods of illuminating the resonator were tested. The straight-through method of the first experiment did not work well when the membrane reflectivity was increased because of the absorbance of the metallic coating and grain scattering.

An on-axis mode with a beamsplitter to reflect fringes from the mirror side was found to have high background scatter and was wasteful of energy. A folded circulator mode could be set up but the finesse was poor because of the many extra reflections from the collodion surface. We finally settled on the biprism corrector described previously.

On the basis of these experiments, we constructed the resonator microphone of Figure 7. It is suitable for mounting on the sound exit port of the acoustic sample chamber. There is one adjusting screw to bring the mirror to the confocal position and another to move both the mirror and the membrane to the sound focus. Two micrometers provide orthogonal fine adjustment of the mirror attitude. The membrane is mounted at a spacing of 1 mm between two wire grids. The grids, which ordinarily are parts of microwave tubes, consist of tungsten wires 0.0003 inch in diameter spaced to cover 1 percent of the surface area.

4.3 THE ACOUSTIC CHAMBER

The acoustic chamber is an evacuable chamber that retains the gas sample and provides for aligned mounting of the acoustic reflectors. The tank could be evacuated down to 10^{-2} mm Hg (1.3 N/M^2), which is sufficient evacuation to insure purity of samples. The mirrors were machined as parabolas to a 0.005 inch tolerance, which is less than 1/10 of a sound wavelength at 300 kHz. Ambient sound in the closed tank is about 30 db.

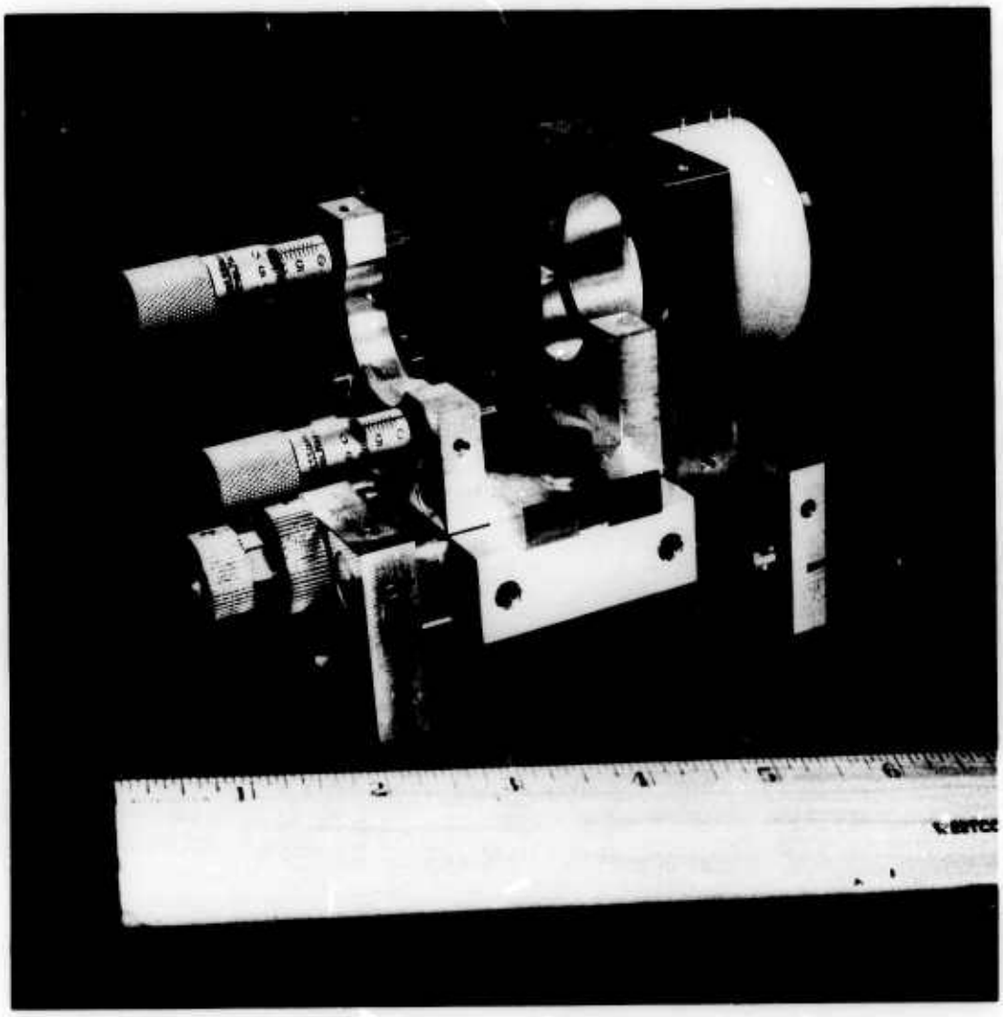

Figure 7. New Force Balance Microphone

4.4 WAVELENGTH CALIBRATION

We used the frequency stable gas laser as an unchanging wavelength standard. It was set to the Lamb dip by adjustment of the pusher mirror. The ruby laser rings and the gas laser rings are recorded side by side on the same film for every pulse, as in Figure 8. The wavelength measuring system is shown in Figure 9.

4.5 EXPERIMENTS WITH AN AUDIO FREQUENCY CERAMIC MICROPHONE

The basic wavelength of the acoustic signal is twice the diameter of the pulsed laser beam. This corresponds to a frequency of 300 kHz. While the high bandwidth membrane microphone was being tested, we placed a ceramic microphone of 10 kHz bandwidth at the acoustic chamber sound focus. Our intention was to check for disruptive, spurious sounds, associated with firing of the pulsed laser, that could possibly mask the acoustic signal due to light absorption. Figure 10 shows a typical response signal. The sweep was started when the Q-switched pulse was detected by a photodiode. The pulsed laser was about 2 meters from the tank. Both were clamped to a massive iron table. During the first 2 milliseconds, no signal is observed.

During the third millisecond, a 5 kHz vibration starts. After about 5 milliseconds we observe a 1 kHz vibration and a 200 Hz vibration. The 5 kHz vibration may be attributed to sound generated in the ruby laser and conducted through the table. The lower frequency vibrations appear to be the tank impulse response to airborne sound. In any case, there are no significant disturbances at 1.5 milliseconds, which is the time the acoustic signal is expected to arrive at the sound focus.

This experiment also gives an upper bound on the strength of any absorption signal that may be present. Use of a 10 kHz bandwidth microphone to detect the laser sound signal leads to a loss of 27 db for frequency mismatch. There is a mismatch of about a factor of 10 between the area of the ceramic microphone and the sound focus spot size, leading to a 20 db loss. There is also a 12 db propagation loss in the tank. The ambient noise in

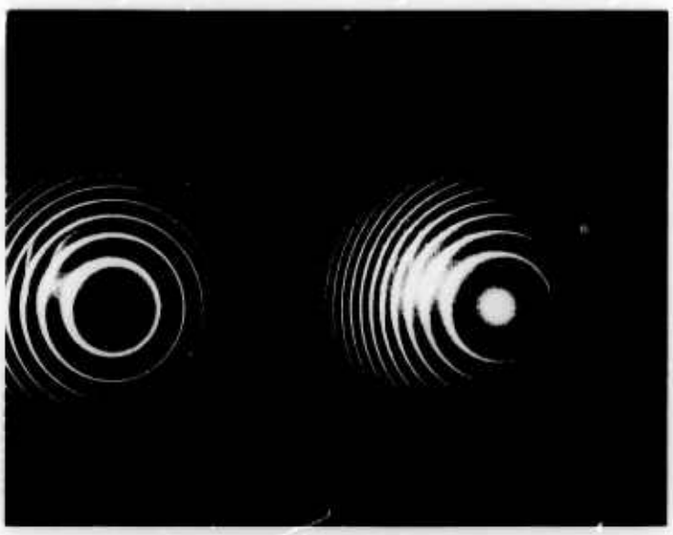

Etalon Spacing
5mm

Ruby He-Ne

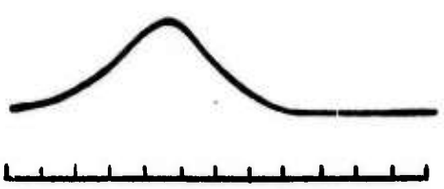

Scale: 1 division = 10 nanoseconds

Figure 8. Typical Calibration Photo and Laser Shot

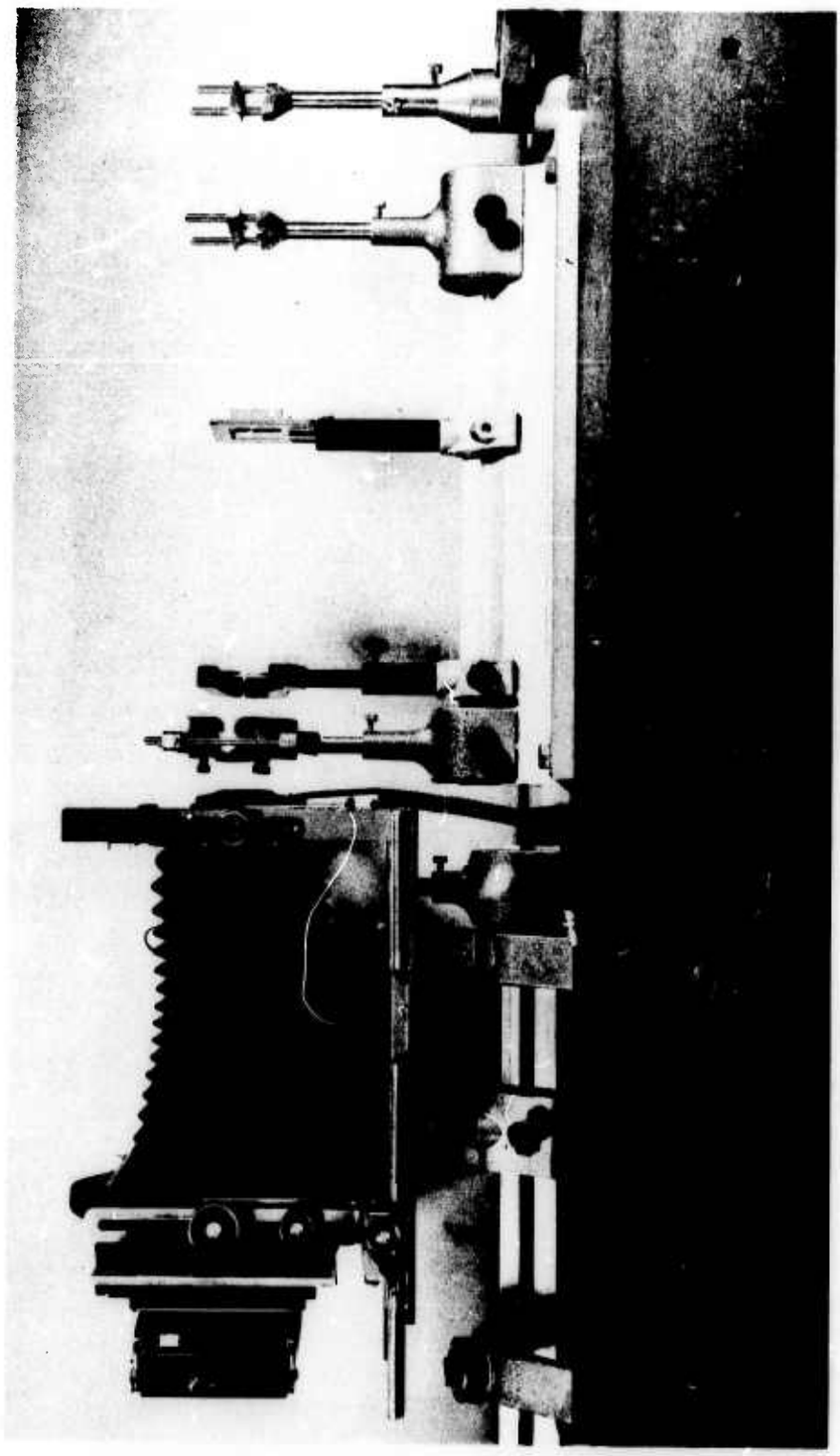

Figure 9. Wavelength Measuring System

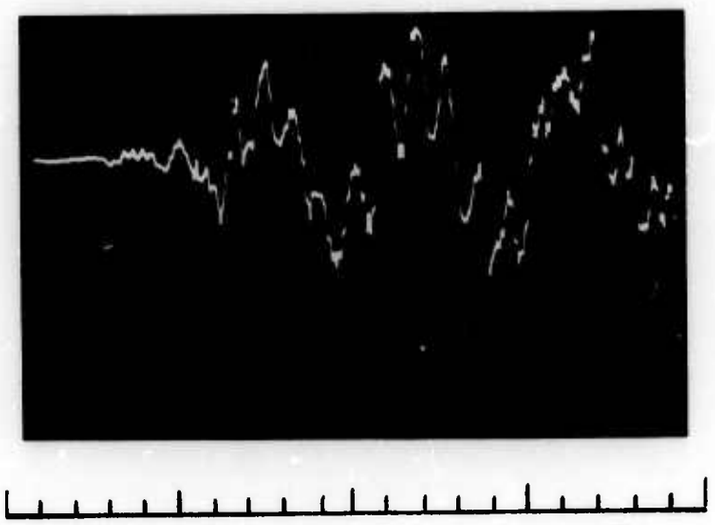

Time Scale: 1 division = 1 millisecond

Figure 10. Typical Response With 10kHz Microphone

the tank was about 35 db at the time these data were taken. Hence, a pressure signal as great as 94 db would go undetected with the ceramic microphone as the sensor. An absorption of 10^{-6}/cm with a 50 millijoule pulse would make a pressure signal of 90 db. Hence, the high bandwidth and sensitivity of the membrane microphone are required.

4.6 CAPABILITY OF THE SECOND MEMBRANE MICROPHONE

We put the new membrane microphone into a vacuum-tight antechamber attached to the original sample chamber. The first tests showed that noise caused displacements of 1/2 order, or about 800Å, making this the smallest detectable signal displacement. The room noise was reduced to a suitable level by the shielding of the tank. Most of the noise was shot noise in the photocells, or oscillations in the servo loop set off by table vibrations. We made many small adjustments in optical alignment and improved the light level considerably. We matched the resonator mirror reflectivity to the membrane reflectivity, sacrificing finesse to fringe visibility. As the noise was reduced, it was possible to increase the loop gain without starting oscillations. Several baffles were required to prevent light scattered by the ruby laser flash from entering the microphone photomultiplier tubes. Eventually we were able to obtain a servo system in which noise represented about 1/10 to 1/20 of a resonator order. The system was stable for several seconds, during the disturbance of the pulse laser flash. This made displacements of about 160Å detectable.

Many data were taken on the membrane resonances, because the servo stability is upset by resonance and because the membrane tension can be calculated from the fundamental resonance frequency. The membrane tension for collodion is usually about 10^4 dynes-cm^{-1}. Thus, a static pressure of about 0.1 dyne cm^{-2} could be detected. At high frequencies, the membrane does not respond to pressure but rather to displacements of the medium to which it is coupled.

4.7 RECIPROCITY EXPERIMENTS

Some attempt was made to use the microphone as a reciprocal device. A voltage pulse applied to the wire grids forcefully attracts the membrane, producing a sound pulse. A solid bar or wire placed along the path of the pulse laser light will reflect the sound wave. The returning echo can be detected by the microphone. In most of the tests, however, the returning echo was lost in noise because of the high attenuation along the beam path and the scattering losses at the reflecting bar.

4.8 ABSORPTION EXPERIMENTS WITH THE ACOUSTIC METHOD

In spite of the disappointing performance of the membrane microphone in detecting high frequency signals, we tried to find any signal at all which could be identified as an absorption signal. We felt that if a strong absorption could be detected, the system could be improved to detect weaker signals. However, there are very few gases which absorb strongly near 6943Å, and most of them are corrosive. Construction of corrosion-proof apparatus was not justified at this point. No signals that could be positively identified as being due to water vapor absorption were observed.

SECTION V

EVALUATION OF THE ACOUSTIC METHOD

The acoustic method, in which the sound pulse generated by absorbed light energy is focused on a membrane microphone detector, cannot reach theoretical limits of performance because of the interrelated practical problems of:

a. The small free sound field displacement at high frequencies.

b. The conflicting requirements of small membrane mass for good acoustic coupling and high membrane reflectivity for adequate finesse.

c. The short observation time which makes shot noise, rather than acoustic thermal noise, the limiting noise in the optical measuring apparatus.

The best experimental results obtained with the acoustic method indicated sensitivity such that a 10^{-5} cm^{-1} absorptivity could have been detected with a 50 millijoule pulse. We had no noncorrosive gas with this great an absorptivity to make the test, however. The minimum detectable membrane motion was about 1/2 a fringe, or 800Å, because of shot noise.

The method will still be useful for studying molecular absorption relaxation times, since it affords an extremely short response time. To use it in this way, however, will require strongly absorbing samples and Q-switched laser frequencies to match them. It will also probably require better membrane materials and/or a higher power source.

REFERENCES

[1] Harold D. Babcock and Charlotte E. Moore, "The Solar Spectrum, λ6600 to λ13495," Carnegie Institute of Washington, Publication 579, Washington, D.C., 1947.

[2] J.A. Curcio, L.F. Drummeter, and G.L. Knestrick, "An Atlas of the Absorption Spectrum of the Lower Atmosphere from 5400Å to 8520Å," Applied Optics, Vol. 3, No. 12, (December, 1964), pp. 1401-1409.

[3] Ronald K. Long, "Atmospheric Attenuation of Ruby Lasers," Proceedings of the IEEE, Vol. 51, No. 5, (May, 1963), p. 859.

[4] Ronald K. Long, Absorption of Laser Radiation in the Atmosphere, Ohio State University, May 31, 1963. AD 410571.

[5] W.H. Culver, "Precision, Absolute Measurement of the Optical Absorption Spectra of Gases," Journal of Applied Physics, Vol. 35, No. 11, (November, 1964), p. 3421.

APPENDIX A

STATEMENT OF WORK

APPENDIX A

STATEMENT OF WORK

Perkin-Elmer shall furnish the necessary personnel and facilities for and, in accordance with any instructions issued by the Scientific Officer or his authorized representative, shall design and build the necessary experimental equipment to evaluate the acoustic method for measuring optical absorption in gases. The experiments will be carried out, and data will be obtained, for air and some test gases at not less than one laser wavelength region.

Perkin-Elmer shall also evaluate the acoustic and spectrophone methods for measuring optical absorption in gases.

LIST OF TECHNICAL AND ADMINISTRATIVE REPORTS SUBMITTED

First Quarterly Letter Report through 31 December 1964, February 26, 1965

Second Quarterly Letter Report through 31 March 1965, April 6, 1965

First Semiannual Technical Summary Report through 31 March 1965 (Perkin-Elmer Report No. 8011)

Third Quarterly Letter Report through 30 June 1965, 10 July 1965

Fourth Quarterly Letter Report through 30 September 1965, 10 October 1965

First Annual Technical Summary Report through 31 January 1966 (Perkin-Elmer Report No. 8361)

Fifth Quarterly Letter Report through 30 September 1966 (Perkin-Elmer Report No. 8550)

Second Semiannual Technical Summary Report through 31 December 1966 (Perkin-Elmer Report No. 8670)

Sixth Quarterly Letter Report through 31 March 1967 (Perkin-Elmer Report No. 8741)

Final Report through 31 July 1967 (Perkin-Elmer Report No. 8884)

PATENT ACTION

We applied for patent on the force balance microphone described in Section IV.

The Perkin-Elmer Patent Law Department is processing disclosures on a Series Etalon System for high resolution, low ambiguity wavelength measurement, and on the absorptivity spectrophone system.

APPENDIX B

THE ABSORPTIVITY SPECTROPHONE - A PRACTICAL, DIRECT METHOD FOR PRECISE MEASUREMENT OF WEAK OPTICAL ABSORPTIVITY IN GASES

We expect to publish this article along with Appendix C. Figures 4 and 5 will not be part of the article. They illustrate the CO_2 laser excited absorptivity spectrophone described in the last section of this article.

This article represents our evaluation of the spectrophone method. In summary, the absorptivity spectrophone is a simple, inexpensive, precise, proven system suitable for a survey of very weak atmospheric absorptivities in the tuning region (if any) of a high power laser.

The Absorptivity Spectrophone - A Practical, Direct Method for Precise Measurement of Weak Optical Absorptivity in Gases

EDWIN L. KERR AND JOHN G. ATWOOD
The Perkin-Elmer Corporation, Norwalk, Connecticut

ABSTRACT

A spectrophone measures absorptivity by sensing thermal expansion in a confined sample gas. Laser source excitation provides sufficient radiation to measure very weak absorptivities precisely. This paper describes the theoretical capability, design considerations, and experimental testing of a pulsed ruby laser absorptivity spectrophone and a CW CO_2 absorptivity spectrophone. A spectrum of the water vapor line at 6943.8Å was obtained. The peak absorptivity was $3 \times 10^{-6} cm^{-1}$. In the region of 9.6μ, absorptivities of CO_2 - N_2 mixtures were measured down to $1.2 \times 10^{-7} cm^{-1}$.

Interest in gas absorptivities as weak as 10^{-7} cm^{-1} has been stimulated by the development of laser communications and radar systems. They study of two-photon absorption processes in gases requires measurements to 10^{-9} cm^{-1}. Other applications require the location of atmospheric windows with very weak absorptivities. This article describes a laser excited spectrophone,[1] an experimental system which has measured gas absorptivities of 10^{-6} cm^{-1} with a pulsed ruby source laser, and 10^{-7} cm^{-1} with a CW CO_2 laser. With some simple refinements of our first spectrophone breadboards, we believe the system is capable of measuring absorptivities of 10^{-8} cm^{-1} to within ±10%.

With conventional differencing absorbance spectrometers using long path cells, broad-band absorptivities are difficult to distinguish from baseline drift. The absorptivity spectrophone system, described here, avoids this problem since its signal is proportional to absorptivity.

The measured absorptivity is true absorptivity, even in the presence of overwhelming scattering.

THE ABSORPTIVITY SPECTROPHONE SYSTEM

Figure 1 shows the general layout of the absorptivity spectrophone system. The main features are:

1. A pulsed or CW coherent source
2. A short, single-pass gas sample cell
3. A low-frequency differential pressure transducer

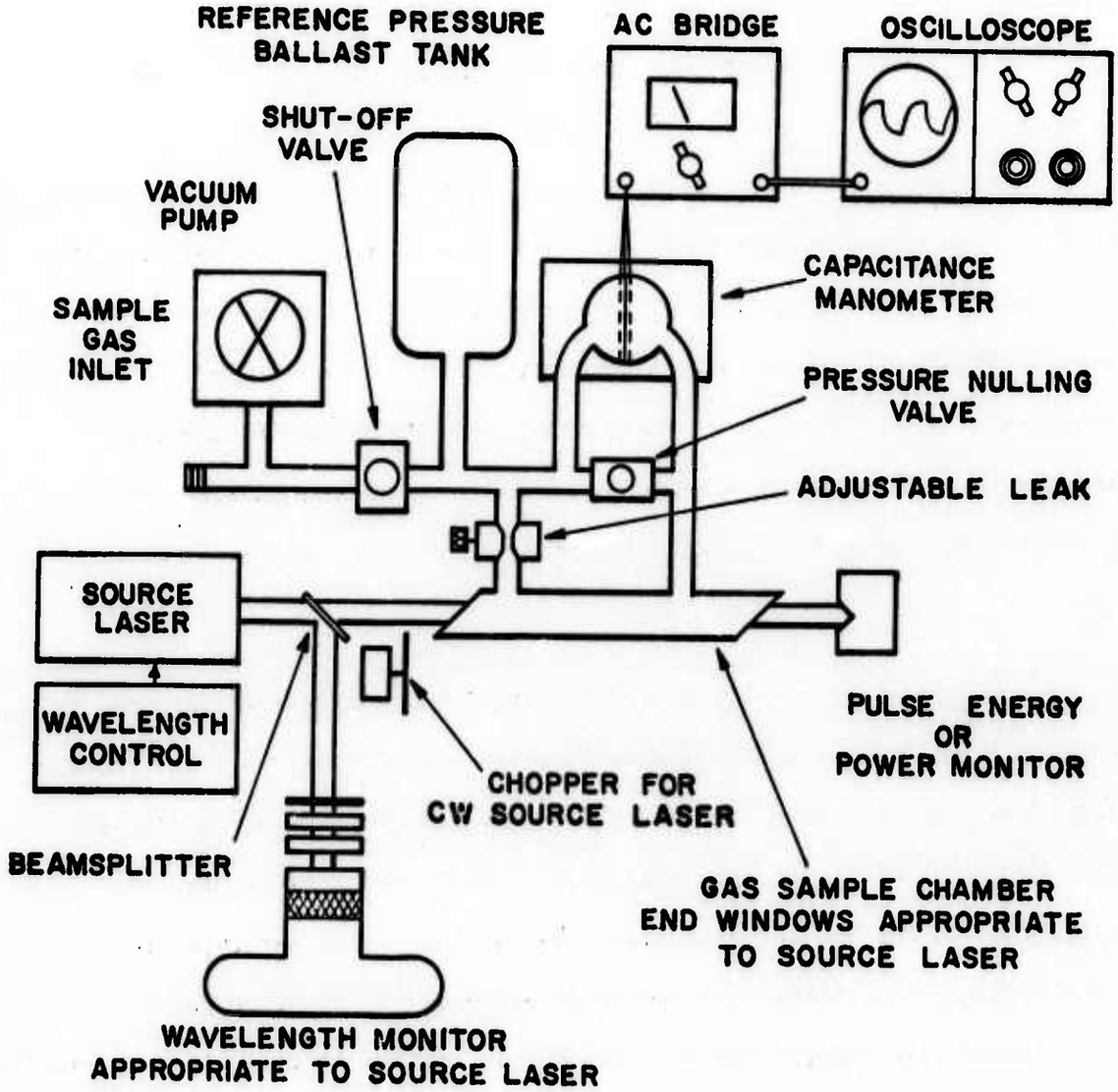

Figure 1. The Absorptivity Spectrophone Apparatus for Measurement of Weak Optical Absorptivities in Gases

The coherent source is not required to be particularly stable or repeatable. Good results can be obtained even with large source power fluctuations which would be intolerable in conventional absorbance spectrometers. Tunability is necessary for obtaining a spectrum. Other applications may require little or no tunability. Several types of lasers can be tuned over short ranges. For example, the wavelength of a ruby source laser can be shifted from 6938Å through 6943Å by controlling the ruby temperature. The various rotational lines of the CO_2 laser can be selected by using a dispersive element in the laser cavity and active cavity length stabilization. Some other types of source lasers can be tuned slightly by adjusting the laser cavity length. The wavelength is measured with etalons or monochrometers. Appropriate calorimeters or thermopiles monitor the laser pulse energy or power.

In the sample cell, energy absorbed from the beam is degraded to thermal motion. The resulting pressure rise is proportional to the molecular absorptivity. For a pulsed source laser, the pressure observation time is limited by heat diffusion to the cell walls. For a CW source laser, the chopping rate is chosen slow enough so that, during each illumination cycle, heat conduction establishes a steady temperature distribution in the gas. The adjustable leak compensates for the average heating of the cell over many cycles or pulses and prevents long-term pressure buildup. The sample cell calibration depends only on its geometry.

The minimum detectable pressure required is many decibels above thermal agitation noise levels. A calibrated, sealed capacitance manometer is appropriate. In our experiments, we used the MKS Baratron. It has a thin

sealed stretched steel diaphragm and a calibrated AC bridge for capacitance readout. The response time is less than 100 milliseconds to a pressure step. The maximum pressure range was 10 mm Hg, or 1 mm Hg, depending on which interchangeable pressure head was used. The smallest scale division is 10^{-5} of the maximum range.

THEORETICAL CAPABILITY

The theoretical signal-to-noise ratio can be calculated by comparing the signal pressure amplitude with Brownian noise pressure. As we shall see, this does not set the system performance limit. The thermal stability problem is by far the more stringent requirement in the practical system.

The root-mean-square Brownian noise pressure is 7.6×10^{-8} dynes cm^{-2} for air at one atmosphere and room temperature, when the upper cutoff frequency is 100 Hz.

If the average temperature fluctuation of the sample cell during illumination is to cause pressure changes comparable with rms Brownian noise, the thermal stability required during the observation time is 2×10^{-11}°C! A much more reasonable goal for a practical system is to measure pressure rises as small as 1 dyne cm^{-2} ±10%. Then the cell's average temperature fluctuation can be $\pm 3 \times 10^{-5}$°C over the observation time.

TYPICAL CASES

In using a pulsed laser spectrophone, the gas absorptivity can be calculated from the measured pressure amplitude, A, according to:

$$\alpha = A\rho c_v T\pi w^2 F/EP$$

This formula is derivable from the amount of heat deposited in the cell by absorption, and ideal gas calorimetry. We assume the heat deposition time is short compared with the thermal decay time constant.

A typical case for a non-Q-switched pulsed ruby laser is pulse energy E = 0.5 joule, nominal sample pressure P = 10^6 dyne cm^{-2} (1 atmosphere), heat capacity ρc_v = 10^{-3} joule $°C^{-1}$ cm^{-3}, beam radius w = 0.15 cm, absolute temperature T = 300°K, ratio F of total cell volume to illuminated sample volume = 1.5. With these parameters and a minimum signal pressure amplitude A of 1 dyne cm^{-2}, an absorptivity of 6 x $10^{-8}cm^{-1}$ is measurable. If a Q-switched ruby laser were used to obtain very high spectral purity, the pulse energy might be only 50 millijoules. In that case, absorptivities of 6 x $10^{-7}cm^{-1}$ could still be measured.

For a CW source laser, the absorptivity is calculated as $\alpha = 4\pi KTA/WPB$, where K is the gas thermal conductivity (2.4 x 10^{-4} watt/cm°C for air) and B is a function of the ratio b of beam radius to cell radius. For b = 0.5, B = 0.8. See the appendix for the derivation of this function. At present it is possible to achieve several watts output with argon lasers and several hundred watts output with CO_2 lasers. Let us use W = 10 watts output in this calculation. Then if the minimum signal amplitude is 1 dyne cm^{-2}, an absorptivity of 1.2 x $10^{-7}cm^{-1}$ can be measured.

ABSORPTIVITY CELL CONSTRUCTION

Cell radius: The radius a of the cell determines the thermal time constant of the pressure signal,

$$\tau = a^2/5.76\,\varkappa$$

where $\varkappa$ is the thermal diffusivity.

For pulsed laser excitation, the pressure signal waveform is approximately a sharp pulse with exponential decay. In order to measure 90% of the amplitude of the sharp peak, the decay time constant had to be over 35 times the pressure transducer time constant. Since the upper cutoff frequency of the transducer was 1.6 millisecond, τ = 56 millisecond, and for air with a diffusivity of 0.26cm^2 second^{-1}, the tube radius should be 3 mm. We chose 4.5 mm to facilitate alignment of the laser beam.

For CW laser excitation, the best choice of thermal time constant would match the pressure transducer time constant, since a longer time constant needlessly complicates the thermal stability problem. The time constant to reach the steady temperature distribution is about 1.2τ. Allowing three time constants to reach the steady pressure during the illumination half-cycle, the chopping frequency is $f = 1/7.2\tau$.

The cell radius must fit the beam closely enough to prevent convection currents. The threshold for onset of convection may be estimated by using Rayleigh's[2] formula:

$$\Delta\rho/\rho > 27\pi^4\,\varkappa\,\eta/4\,ga^3\rho$$

where η is the gas viscosity and g is the acceleration of gravity.

Cell length: In this system, the absorptivity signal is independent of path length. Hence, a moderate cell length is required only to reduce the effects of end window heating, and to make the volume of the sample gas in the beam path much greater than the unilluminated volume in the sample inlet tubes and the pressure transducer. Although the maximum cell length is set by the laser beam divergence, in practice a much shorter cell sufficed.

Thermal stability: Absorption of light in and at the sample cell end windows warms the cell, heats the sample gas, and gives a false pressure reading. The window heating effect may be reduced by providing good thermal contact with the cell and by making the cell very massive near the windows. The cell wall should also be massive for general thermal stability. A rough estimate of the useful wall thickness is obtained from a standard one-dimensional heat flow problem in which the edge temperature of a semi-infinite slab is suddenly raised above ambient[3]. The distance to the point with 10% of the surface temperature is

$$x = 2.4\ (\varkappa t)^{1/2}$$

where here $\varkappa$ is the thermal diffusivity of the cell wall material, and t is the observation time.

The leak had a time constant about 10 times longer than the system response time, for the pulse method. In the CW method, the leak was adjusted to give a flat-top response to the square wave heating input.

EXPERIMENTAL RESULTS: THE RUBY LASER ABSORPTIVITY SPECTROPHONE

An absorptivity spectrophone breadboard excited by a small ruby laser was constructed. Even though the system was far from optimum, absorptivities of 10^{-6} cm^{-1} were measured.

The source laser was a 0.25 inch diameter x 3 inch long ruby with external plane mirrors of 50% and approximately 100% reflectivity. Methanol and water was circulated through a quartz coolant jacket surrounding the ruby, inside the coils of the helical xenon flash lamp. A two-liter reservoir provided enough thermal inertia to cause slow wavelength scanning when the laser was pulsed every 80 seconds. Non-Q-switched pulses of 300 to 400 millijoules were obtained with 7 kilojoules input energy. A calorimeter and a 1 cm^{-1} etalon monitored the pulse energy and wavelength. The wavelength spread was 0.2Å in each pulse.

The sample chamber was a glass tube 45.5 cm long by 4.5 mm inside diameter, with light borosilicate crown glass (BK-7) end windows at Brewster's angle. An iris limited the beam diameter to 3mm. The Baratron pressure transducer used had a maximum range of 10 mm Hg. The volume reduction factor was 20 because of several inlet tubes and about 5 cm^3 volume in the pressure transducer. The leak was a capillary tube with a 3 second time constant. Acoustic and thermal shielding was provided by housing the sample tube within a pressure tank.

Figure 2 shows the water vapor line at 6943.8Å. The sample was air saturated with water vapor at room temperature. Each point represents a single pulse. The noise level is high because the glass sample cell was not sufficiently massive to prevent a large temperature rise at the end windows. Only the relative wavelength was measured with the etalon, but the ruby temperature, ranging from 15°C to 37°C, was recorded. This is sufficient to identify the line from solar spectra.[4]

EXPERIMENTAL RESULTS: THE CO_2 LASER ABSORPTIVITY SPECTROPHONE

A CW absorptivity spectrophone for use with a 10 watt CO_2 laser was breadboarded. Its sensitivity permitted measurements down to a threshold of $5 \times 10^{-8} cm^{-1}$.

The CO_2 laser was DC excited, water cooled, 1.4 meter long, 1 cm in diameter, with a plane-spherical cavity. The spherical mirror was coated to discriminate against the 10.6μ band, so the laser operated in the region of 9.6μ without wavelength control. Input power was 500 watts.

The sample cell was aluminum, 2 cm ID, 10 cm OD, 20 cm path length, 4.2 kg mass and had 6 mm thick salt windows at Brewster's angle. We tried NaCl, CsI, and CsBr windows, but found that KBr windows gave the smallest false pressure signals. Dry nitrogen purging, vacuum pumping, and bakeout to 100°C removed most of the contaminants, but enough remained to give an equivalent absorptivity of $5 \times 10^{-8} cm^{-1}$ with dry N_2 at atmospheric pressure in the cell. The source of false signals was probably water vapor

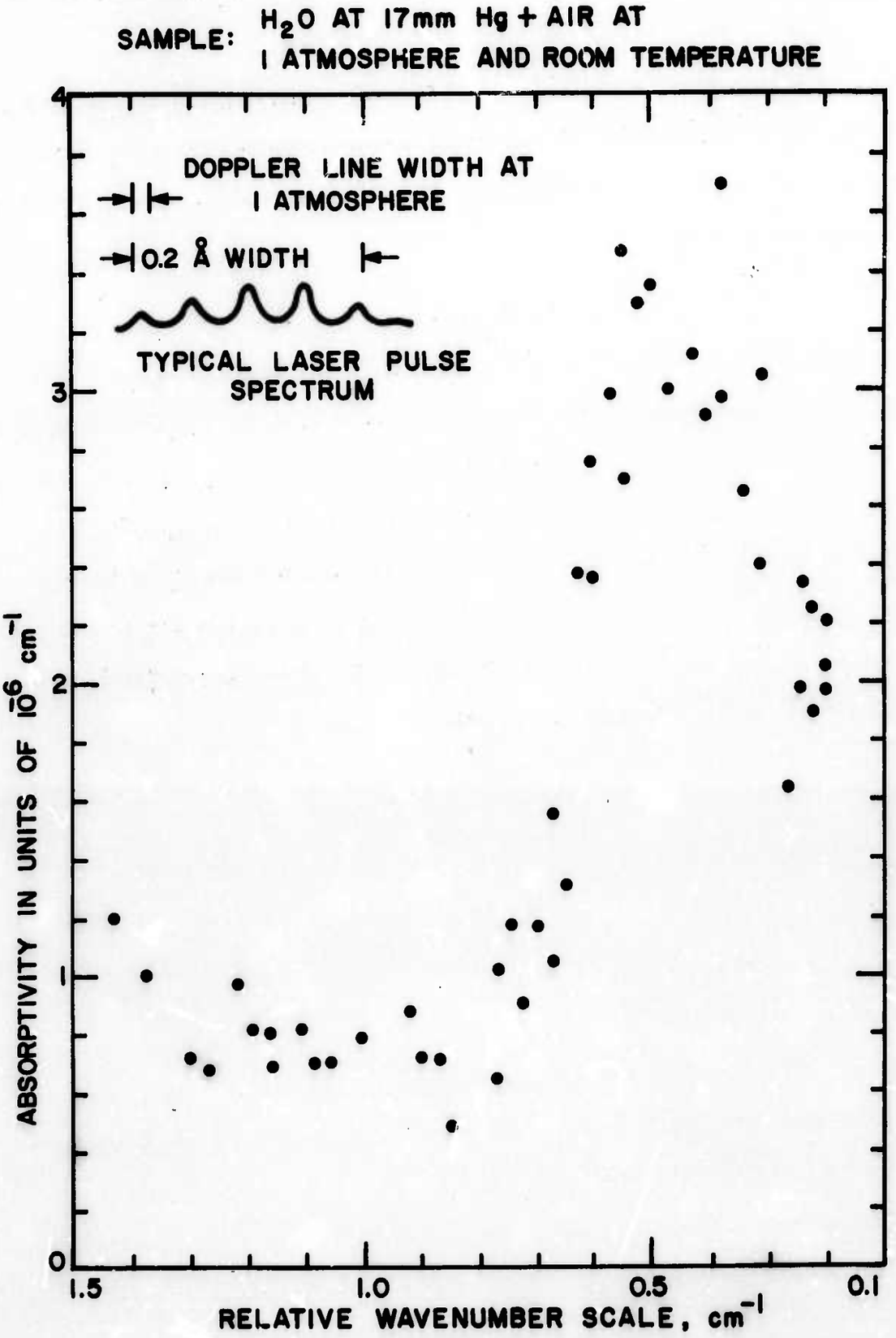

Figure 2. H_2O Vapor Absorption Line at 6943.80Å

clinging to the hygroscopic salt windows. Future cells should be designed to allow dry N_2 flow in sheets across the window for purging. Because of the large tube radius necessary to pass the laser beam without lenses, the chopping frequency was 0.19 Hz.

A more sensitive Baratron pressure transducer was used, with a maximum range of ±1 mm Hg, a resolvable differential of 0.01μ Hg, and only 0.75 cm^3 internal volume.[5] The system was tested by measuring the absorptivity of CO_2 - N_2 mixtures, on the assumption that the N_2 has negligible absorptivity near 9.6μ. The absorptivity of pure CO_2 at 1 atmosphere was measured as 1.35×10^{-3} cm^{-1}. The absorptivity of CO_2 - N_2 mixtures was found to be linear with CO_2 concentration down to 66 ppm CO_2. In particular, at 300 ppm CO_2 (the standard concentration of CO_2 in air at sea level) the absorptivity was $5.8 \times 10^{-7} cm^{-1}$. The data are plotted in Figure 3.

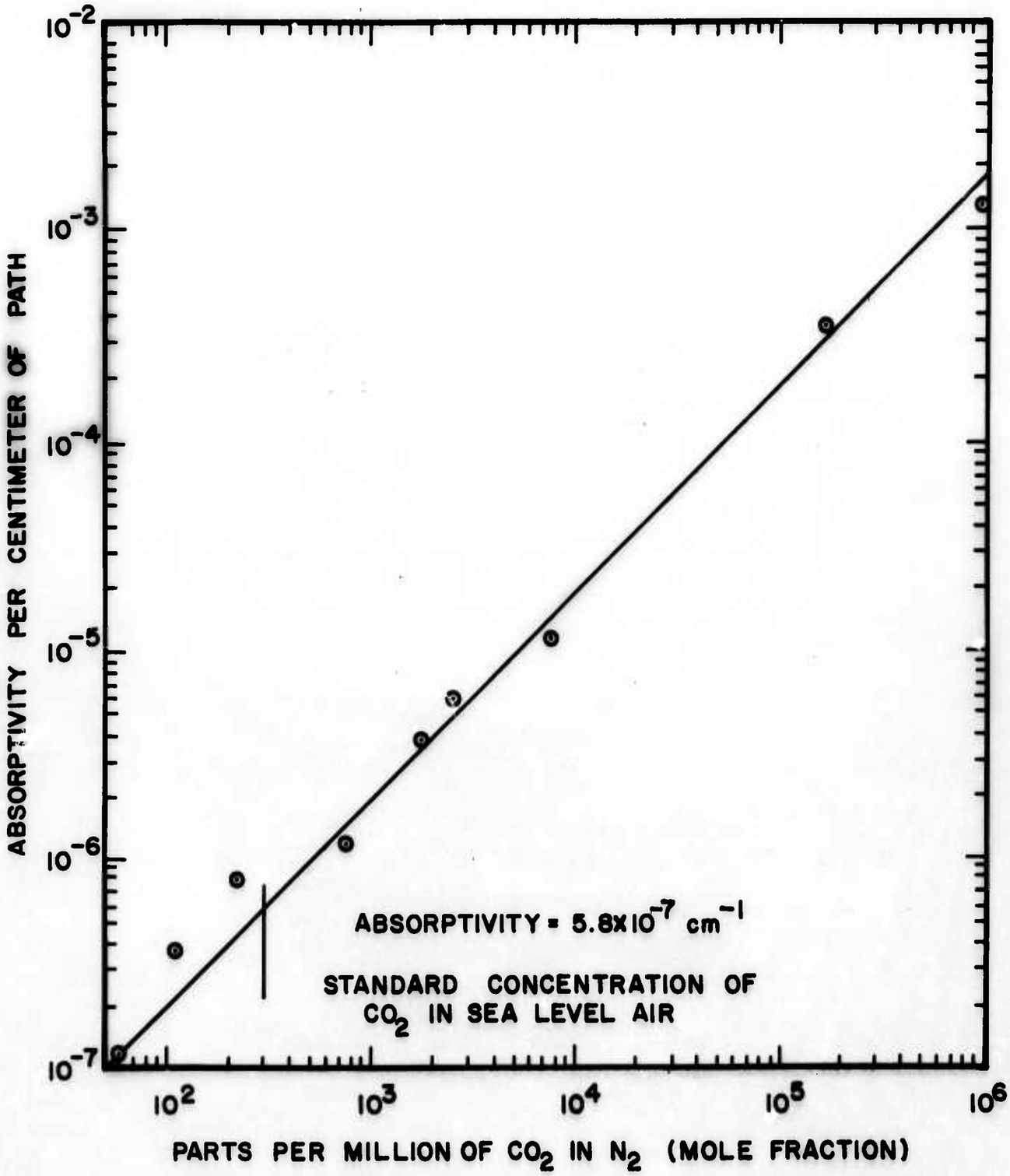

Figure 3. Absorptivity Near 9.6μ of CO_2 - N_2 Mixtures

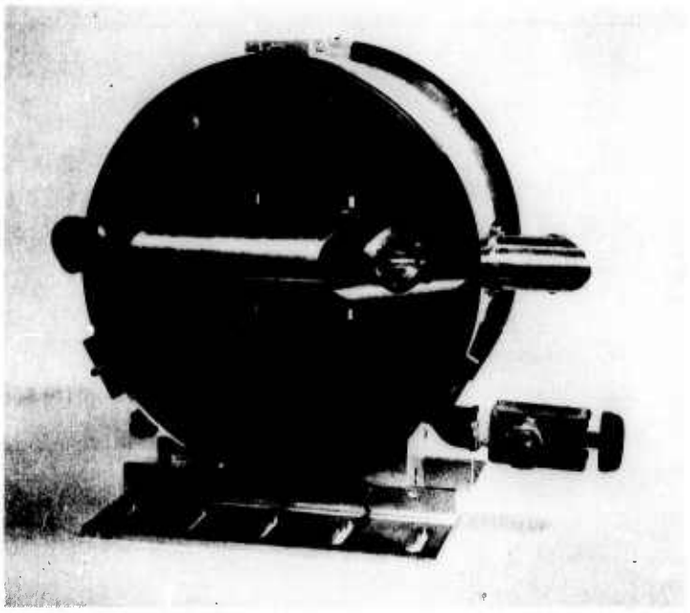

Figure 4. Massive Sample Cell and Pressure Tank For Use Near 9.6μ

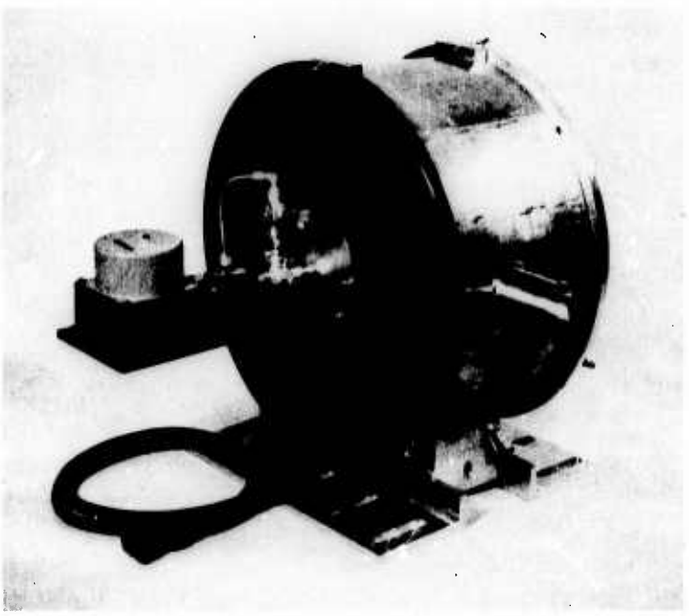

Figure 5. The MKS Baratron Attached to the Pressure Tank. The Micrometer Valve is the Adjustable Leak.

REFERENCES

1. Earlier spectrophones have been used to measure relaxation times. See P.V. Slobodskaia and E.S. Gasilevich, Optika i Spektroskopiia, 7, 97(1959); 8, 678(1960); "Development of a Method of Determining the Relaxation Time of the Vibratory State of Molecules Using a Spectrophone. I. Establishment of a More Accurate Dependence Between the Measured Phase Shift and Relaxation Time." Optics and Spectroscopy, 7, 58-62(1959); "Development of a Method for Determining Relaxation Time Using a Spectrophone. II. Eliminating the Instrumental Phase Shifts." 8, 358-362(1960); and P.V. Slobodskaia; "Study of the Relaxation Time of the Vibrational State Corresponding to the 4.3nm Absorption Band of Carbon Dioxide by Means of a Spectrophone." Optics and Spectroscopy, 22, 14-17(1967).

2. John William Strutt, Lord Rayleigh, "On Convection Currents in a Horizontal Layer of Fluid, When the Higher Temperature is on the Under Side," Scientific Papers, Cambridge (1920) 6, 432-446.

3. The problem is worked out by Ian N. Sneddon, Fourier Transforms, McGraw-Hill (1951), 167-170.

4. For an atmospheric spectrum in this region, see Ronald K. Long, "Atmospheric Attenuation of Ruby Lasers." Proceedings of the IEEE, 51, No. 5, p. 859 (May 1963).

5. The manufacturer's calibration was spot-checked and found to be accurate.

APPENDIX C

THE ABSORPTION CELL PRESSURE RESPONSE TO A GAUSSIAN DISTRIBUTED SOURCE BEAM

APPENDIX

THE ABSORPTION CELL PRESSURE RESPONSE TO A GAUSSIAN DISTRIBUTED SOURCE BEAM

The average pressure rise in the absorption cell can be calculated from the temperature distribution and the ideal gas law. In this analysis the gas absorptivity may be determined from the average pressure rise if the thermal conductivity is known. The thermal diffusivity can be found from the initial rate of pressure rise.

COORDINATES AND GEOMETRY OF THE HEAT FLOW PROBLEM

Assume the cell is long and thin, so heat loss through the end windows is small compared with heat loss to the walls. Let the laser beam have a gaussian intensity distribution and cylindrical symmetry. This reduces the problem to one-dimensional heat flow.

Let a = cell radius

Let $I'(\rho)$ = beam intensity distribution

$$I'(\rho) = (W/\pi w^2) \exp(-\rho^2/w^2)$$

where W = beam power,

w = beam spread (half-width at e^{-1} points).

Let $r = \rho/a$ = dimensionless radial coordinate.

Thus the dimensionless cell radius is 1.

Let $b = w/a$, the fraction of the cell radius occupied by the beam.

$$\text{Thus } I'(r) = (W/\pi a^2 b^2) \exp(-r^2/b^2).$$

The intensity at the cell walls is $(W/\pi a^2 b^2) \exp(-1/b^2)$. It is desirable to have an intensity distribution which becomes 0 at r = 1. Hence, define a new intensity distribution.

$$I(r) = (W/\pi a^2 b^2)\left[\exp(-r^2/b^2) - \exp(-1/b^2)\right].$$

When $b \ll 1$, the intensity is only slightly reduced, but the heat flow problem is made much more tractable by eliminating infinite gradients at the tube walls.

Let α = gas absorptivity per unit length. Assume $\alpha \ll 1$, so the absorbed power per unit length is αW.

Let A = rate of heat generation per unit volume per unit length in the cell. Let the unit volume be $a^2 \cdot 1$ unit length, so

$$A(r) = (\alpha W/\pi b^2)\left[\exp(-r^2/b^2) - \exp(-1/b^2)\right].$$

SEPARATION OF THE HEAT FLOW PROBLEM

Let $\theta = \theta(r,t)$ = temperature in the cell above ambient temperature.

The heat flow equation is

$$\partial^2 \theta/\partial r^2 + r^{-1}\,\partial\,\theta/\partial r = a^2 \varkappa^{-1} \partial\theta/\partial t - A(r)/K$$

where $\varkappa$ = gas thermal diffusivity = $K/\rho C_v$

K = gas thermal conductivity

ρ = gas density

C_v = gas specific heat capacity at constant volume

Initial condition: $\theta(r,o) = 0$

Boundary conditions: $\theta(1,t) = 0$, $\theta(o,t) \neq \infty$

The first boundary condition is justified because the cell walls have a much higher heat capacity than the gas. The second boundary condition is required on physical grounds.

The heat flow problem may be separated into the steady-state solution and the transient solution. Let $\theta = u(r,t) + v(r)$. Then v satisfies the steady-state equation

$$d^2v/dr^2 + r^{-1}dv/dr = -A(r)/K$$

subject to $v(o) \neq \infty$, $v(1) = 0$. Also u satisfies the transient solution equation

$$\partial^2u/\partial r^2 + r^{-1}\partial u/\partial r = a^2\kappa^{-1}\partial u/\partial t$$

subject to $u(o,t) \neq \infty$, $u(1,t) = 0$

and $u(r,o) = -v(r)$. Obviously the steady-state problem must be solved first.

THE STEADY-STATE TEMPERATURE DISTRIBUTION

Multiplying the steady-state equation by r, we have

$$d(r\, d\, v/dr)/dr = -(\alpha W/K\pi b^2)r\left[\exp(-r^2/b^2) - \exp(-1/b^2)\right].$$

Integrating and dividing by r, we obtain

$$dv/dr = (\alpha W/K\pi)\left[\exp(-r^2/b^2)/2\, r + .\exp(-1/b^2)r/2b^2\right] + C_1/r.$$

The first exponential factor can be integrated term by term. Replace it with

$$1/2r + (1/2)\sum_{n=1}^{\infty}(-1)^n\, r^{2n-1}/b^{2n}n!$$

and integrate to obtain

$$v = (\alpha W/K\pi)\left[(1/4)\sum_{n=1}^{\infty}(-1)^n(r/b)^{2n}/nn! + (1/2)\ln r + (r^2/4b^2)\exp(-1/b^2)\right] + C_1 \ln r + C_2.$$

To satisfy $v(o) \neq \infty$, let $C_1 = -\alpha W/2K\pi$

To satisfy $v(1) = 0$, choose C_2 so

$$v = (\alpha W/4\pi K)\left[\sum_{n=1}^{\infty}(-1)^n(r^{2n}-1)/b^{2n}nn! + \exp(-1/b^2)(r^2-1)/b^2\right]$$

THE STEADY-STATE PRESSURE

The relation between the pressure rise and the temperature rise is found by differentiating the ideal gas law,

$dP/P = dT/T$ where P is the nominal pressure and T is the absolute ambient temperature. The average pressure p is found by the integral

$$p_1 = (2\pi \cdot 1 \text{ unit length}/V)(P/T)\int_o^1 v(r)\, r\, dr$$

where the dimensionless volume $V = \pi\, 1^2\, 1$ unit length. Hence

$$p_1 = (2P/T)\int_o^1 v(r)\, r\, dr$$

$$= (\alpha WP/4\pi KT)\left\{\sum_{n=1}^{\infty}(-1)^n\left[r^{2n+2}/(n+1) - r^2\right]/b^{2n}nn! + \exp(-1/b^2)(r^4/2 - r^2)/b^2\right\}_o^1$$

$$= (\alpha WP/4\pi KT)\left[\sum_{n=1}^{\infty}(-1)^{n+1}/b^{2n}(n+1)! - \exp(-1/b^2)/2b^2\right]$$

$$= (\alpha WP/4\pi KT)\left[1-b^2 + \exp(-1/b^2)(b^2-1/2b^2)\right]$$

Let $B = B(b) = \left[1-b^2 + \exp(-1/b^2)(b^2-1/2b^2)\right]$

Then the absorptivity is

$$\alpha = p_2 4\pi KT/WPB(b) \qquad (1)$$

Table I gives values of B for cases of interest. .

TABLE I

b	$\cong 0$	0.20	0.25	0.30
B	1	0.960	0.938	0.910

THE TRANSIENT TEMPERATURE SOLUTION

A solution of the transient temperature solution yields the gas thermal diffusivity in terms of the amplitude and initial slope of the pressure rise.

Assume that $u(r,t) = R(r)\,T(t)$. The heat flow equation becomes

$$R^{-1}(d^2R/dr^2 + r^{-1}\,dR/dr) = a^2\varkappa^{-1}T^{-1}\,dT/dt = -\xi^2$$

where $-\xi^2$ is an arbitrary constant.

The solutions are

$$T = \exp(-\varkappa\,\xi^2 t/a^2) \text{ and}$$

$$R = C\,J_o(\xi r) + DN_o(\xi r)$$

Since $u(o,t) \neq \infty$, $D = 0$. To satisfy $u(1,t) = 0$, chose $\xi = \xi_m$, where ξ_m is the mth root of $J_o(\xi) = 0$.

The general solution so far is

$$u(r,t) = \sum_{m=1}^{\infty} C_m\,J_o(\xi_m r)\exp(-\varkappa\,\xi_m^2\,t/a^2)$$

To satisy the initial condition,

$$u(r,o) = \sum_{m=1}^{\infty} C_m\,J_o(\xi_m r) = -v(r),$$

multiply both sides of the equation by $rJ_o(\xi_k r)$, integrate from 0 to 1, and use the orthogonality properties of the Bessel functions to obtain

$$C_k = -\left[2/J_1^2(\xi_k)\right](\alpha W/4\pi K)\cdot$$

$$\cdot\left[\Sigma_{n=1}^{\infty}(-1)^n(n!nb^{2n})^{-1}\int_o^1 (r^{2n+1}-r)J_o(\xi_k r)dr\right.$$

$$\left. + b^{-2}\exp(-1/b^2)\int_o^1 (r^3-r)J_o(\xi_k r)dr\right]$$

$$= \left[2/J_1(\xi_k)\ \xi_k\right](\alpha W/4\pi K)\cdot$$

$$\cdot\left\{\Sigma_{n=1}^{\infty}(-1)^n(n!nb^{2n})^{-1}\left[1-\left(\xi_k/J_1(\xi_k)\right)\int_o^1 r^{2n+1}J_o(\xi_k r)dr\right]\right.$$

$$\left. + 4\exp(-1/b^2)/b^2\xi_k^2\right\}$$

THE TRANSIENT PRESSURE SOLUTION

The transient pressure may now be determined as before.

$$p_2(t) = (2P/T)\int_o^1 u(r)\, r\, dr$$

$$= (2P/T)\sum_{m=1}^{\infty} C_m J_1(\xi_m)\xi_m^{-1}\exp(-\kappa\ \xi_m^2\ t/a^2)$$

$$= (\alpha WP/4\pi KT)\sum_{m=1}^{\infty} D_m \exp(-\kappa\ \xi_m^2\ t/a^2)$$

where $D_m = (4/\xi_m^2)\left\{4\exp(-1/b^2)/b^2\xi_m^2\right.$

$$\left. + \Sigma_{n=1}^{\infty}(-1)^n\left[1-\left(\xi_m/J_1(\xi_m)\right)\int_o^1 r^{2n+1}J_o(\xi_m r)dr\right]/n!nb^{2n}\right\}$$

The integral in D_m decreases with increasing n and with increasing m. It may be evaluated by successive applications of integration by parts. We found evaluation by direct Simpson integration to be simple and precise. Table II gives the coefficients for m=1 through 20, and for various values of b.

TABLE II

VALUES OF D_m

m \ b	0	0.20	0.25	0.30
1	-1.1080	-1.0358	-1.0123	-0.9728
2	0.1398	0.1045	0.8683	0.0704
3	-0.0455	-0.0211	-0.0141	-0.0084
4	0.0210	0.0056	0.0024	0.0009
5	-0.0116	-0.0010	-0.0004	-0.0001
6	0.0072	0.0004		
7	-0.0048			
8	0.0034			
9	-0.0025			
10	0.0019			
11	-0.0015			
12	0.0012			
13	-0.0010			
14	0.0008			
15	-0.0007			
16	0.0006			
17	-0.0005			
18	0.0004			
19	-0.0004			
20	-0.0003			

THE TOTAL PRESSURE RISE

Let p = total pressure rise = $p_1 + p_2(t)$,

$$p = (\alpha WP/4\pi KT)\left[B(b) + \Sigma_{m=1}^{\infty} D_m \exp(-\varkappa \xi_m^2 t/a^2)\right]$$

Let $P(\infty) = A$, the final amplitude of the step response.

The diffusivity can be obtained from the amplitude and the initial slope. Initial slope = $\dot{p}(o)$

$$= -(\alpha WP/4\pi KT)\varkappa a^{-2}\Sigma_{m=1}^{\infty} D_m \xi_m^2$$

$$= \frac{-\alpha WP/4\pi KT)\ B(b)}{(a^2/\varkappa\xi_1^2)B/\Sigma_{m=1}^{\infty}(-D_m)(\xi_m/\xi_1)^2}$$

$$= \frac{A}{\tau\ C(b)}$$

where τ is the principal time constant

$a^2/(2.4048)^2\varkappa$, and C(b) is a correction factor to give the apparent time constant. The correction factor

$$C(b) = -B(b)/\Sigma_{m=1}^{\infty} D_m(\xi_m/\xi_1)^2,$$

is given in Table III for various values of b.

TABLE III

b	≅0	0.20	0.25	0.30
C	1.48	1.44	1.35	1.32

CONCLUSIONS

The absorptivity is given by

$$\alpha = 4\pi KTA/WPB, \tag{2}$$

where K = gas thermal conductivity

T = ambient gas temperature

A = final amplitude of step response

W = beam power

P = nominal gas pressure

B = a function of b, the ratio of beam radius to cell radius, given in Table A-1.

The thermal diffusivity is given by

$$\kappa = \dot{p}\,(o)\, a^2 C/(2.4048)^2 A, \tag{3}$$

where $\dot{p}(o)$ = the initial rate of pressure rise,

a = cell radius

C = a function of b given in Table A-3.

ACKNOWLEDGEMENTS

The authors gratefully acknowledge the engineering contribution to this project of Sidney Appleman.

This research is part of Project DEFENDER under the joint sponsorship of the Advanced Research Projects Agency, the Office of Naval Research, and the Department of Defense. Contract No. Nonr 4661(00).

Unclassified

Security Classification

DOCUMENT CONTROL DATA - R&D

(Security classification of title, body of abstract and indexing annotation must be entered when the overall report is classified)

1. ORIGINATING ACTIVITY *(Corporate author)*

The Perkin-Elmer Corporation
Electro-Optical Division, Norwalk, Connecticut

2a. REPORT SECURITY CLASSIFICATION
Unclassified

2b. GROUP

3. REPORT TITLE

ABSORPTION OF LIGHT IN GASES

4. DESCRIPTIVE NOTES *(Type of report and inclusive dates)*
Final Report

5. AUTHOR(S) *(Last name, first name, initial)*

Kerr, Edwin L. and
Sloan, Earl L. III

6. REPORT DATE	7a. TOTAL NO. OF PAGES	7b. NO. OF REFS
31 July 1967	61	10

8a. CONTRACT OR GRANT NO.	9a. ORIGINATOR'S REPORT NUMBER(S)
Nonr-4661(00)	PE Engineering Report No. 8884
b. PROJECT NO. 4730	
c. TASK ARPA Order 306	9b. OTHER REPORT NO(S) *(Any other numbers that may be assigned this report)* None
d.	

10. AVAILABILITY LIMITATION NOTICES

"Qualified requestors may obtain copies of this report from DDC."

11. SUPPLEMENTARY NOTES	12. SPONSORING MILITARY ACTIVITY
None	"Project Defender" Advanced Research Project Agency, Office of Naval Research, Department of Defense, Washington, D.C.

13. ABSTRACT

Two methods of measuring optical molecular absorptivities in gases, potentially capable of approaching theoretical sensitivity limits of 10^{-8} cm^{-1} were studied. An acoustic method was pushed experimentally to a sensitivity of 10^{-5} cm^{-1} absorptivity. Practical obstacles to further improvement have been found for the acoustic method. The second method, a laser illuminated "spectrophone", was also investigated. Its performance was much closer to the theoretical limit.

The acoustic method is only suitable for use with a pulsed source laser. We used a Q-switched ruby laser, tunable from pulse to pulse over a 2Å range, as the excitation source. Absorbed light causes a temperature rise and expansion of the gas sample. The expansion starts cylindrically propagating sound disturbances. These are focused by acoustic mirrors onto a membrane detector. The membrane is one reflector of a near confocal resonator, illuminated by a frequency stable gas laser. Small membrane displacements are detected as fringe motion across a sensing prism by two photomultiplier tubes. Large

DD FORM 1 JAN 64 1473

Unclassified

Security Classification

Unclassified

Security Classification

14. KEY WORDS	LINK A		LINK B		LINK C	
	ROLE	WT	ROLE	WT	ROLE	WT
Weak absorption of light Pulsed laser applications CW laser applications Acoustic detectors Confocal Resonator Etalon, Fabry-Perot Spectrophone						

INSTRUCTIONS

1. ORIGINATING ACTIVITY: Enter the name and address of the contractor, subcontractor, grantee, Department of Defense activity or other organization *(corporate author)* issuing the report.

2a. REPORT SECURITY CLASSIFICATION: Enter the overall security classification of the report. Indicate whether "Restricted Data" is included. Marking is to be in accordance with appropriate security regulations.

2b. GROUP: Automatic downgrading is specified in DoD Directive 5200.10 and Armed Forces Industrial Manual. Enter the group number. Also, when applicable, show that optional markings have been used for Group 3 and Group 4 as authorized.

3. REPORT TITLE: Enter the complete report title in all capital letters. Titles in all cases should be unclassified. If a meaningful title cannot be selected without classification, show title classification in all capitals in parenthesis immediately following the title.

4. DESCRIPTIVE NOTES: If appropriate, enter the type of report, e.g., interim, progress, summary, annual, or final. Give the inclusive dates when a specific reporting period is covered.

5. AUTHOR(S): Enter the name(s) of author(s) as shown on or in the report. Enter last name, first name, middle initial. If military, show rank and branch of service. The name of the principal author is an absolute minimum requirement.

6. REPORT DATE: Enter the date of the report as day, month, year, or month, year. If more than one date appears on the report, use date of publication.

7a. TOTAL NUMBER OF PAGES: The total page count should follow normal pagination procedures, i.e., enter the number of pages containing information.

7b. NUMBER OF REFERENCES: Enter the total number of references cited in the report.

8a. CONTRACT OR GRANT NUMBER: If appropriate, enter the applicable number of the contract or grant under which the report was written.

8b, 8c, & 8d. PROJECT NUMBER: Enter the appropriate military department identification, such as project number, subproject number, system numbers, task number, etc.

9a. ORIGINATOR'S REPORT NUMBER(S): Enter the official report number by which the document will be identified and controlled by the originating activity. This number must be unique to this report.

9b. OTHER REPORT NUMBER(S): If the report has been assigned any other report numbers *(either by the originator or by the sponsor)*, also enter this number(s).

10. AVAILABILITY/LIMITATION NOTICES: Enter any limitations on further dissemination of the report, other than those imposed by security classification, using standard statements such as:

(1) "Qualified requesters may obtain copies of this report from DDC."

(2) "Foreign announcement and dissemination of this report by DDC is not authorized."

(3) "U. S. Government agencies may obtain copies of this report directly from DDC. Other qualified DDC users shall request through _____."

(4) "U. S. military agencies may obtain copies of this report directly from DDC. Other qualified users shall request through _____."

(5) "All distribution of this report is controlled. Qualified DDC users shall request through _____."

If the report has been furnished to the Office of Technical Services, Department of Commerce, for sale to the public, indicate this fact and enter the price, if known.

11. SUPPLEMENTARY NOTES: Use for additional explanatory notes.

12. SPONSORING MILITARY ACTIVITY: Enter the name of the departmental project office or laboratory sponsoring *(paying for)* the research and development. Include address.

13. ABSTRACT: Enter an abstract giving a brief and factual summary of the document indicative of the report, even though it may also appear elsewhere in the body of the technical report. If additional space is required, a continuation sheet shall be attached.

It is highly desirable that the abstract of classified reports be unclassified. Each paragraph of the abstract shall end with an indication of the military security classification of the information in the paragraph, represented as *(TS)*, *(S)*, *(C)*, or *(U)*.

There is no limitation on the length of the abstract. However, the suggested length is from 150 to 225 words.

14. KEY WORDS: Key words are technically meaningful terms or short phrases that characterize a report and may be used as index entries for cataloging the report. Key words must be selected so that no security classification is required. Identifiers, such as equipment model designation, trade name, military project code name, geographic location, may be used as key words but will be followed by an indication of technical context. The assignment of links, rules, and weights is optional.

Unclassified

Security Classification

13. ABSTRACT (Continued)

displacements are averted by a servo loop which applies the photomultiplier difference signal to electric grids, forcing the membrane to stay within one order of the resonator. The loop feedback signal is a calibratable measure of the gas optical molecular absorptivity at the wavelength of the ruby laser pulse.

One practical problem of the acoustic method is the high frequency and transient nature of the signal. The longest wavelength is twice the laser beam diameter, so the signal frequencies are 300 kHz and higher. The membrane must be very thin to respond to such high frequencies and its displacement is typically less than 1Å. The membrane reflectivity cannot be made greater than 60 percent, so the resonator fringes have low finesse. These practical difficulties make shot noise in the fringe-reading photometer, rather than Brownian noise, the limit of performance.

In the spectrophone method the gas sample is enclosed in a sealed tube. The gas expansion causes a pressure rise which is transmitted to the pressure transducer through a short duct. High frequency problems are avoided. The observation time is typically 30 milliseconds, set by thermal diffusion from the gas sample to the tube walls. Laser source excitation provides sufficient radiation to measure very weak absorptivities precisely. This report describes the theoretical capability, design considerations, and experimental testing of a pulsed ruby laser spectrophone and a CO CO_2 spectrophone. A spectrum of the water vapor line at 6943.8Å was obtained. The peak absorptivity was 3×10^{-6} cm^{-1}. Near 9.6 microns, absorptivities of CO_2 - N_2 mixtures were measured down to 1.2×10^{-7} cm^{-1}.